small methods
www.small-methods.com

Green Hydrogen Production by Low-Temperature Membrane-Engineered Water Electrolyzers, and Regenerative Fuel Cells

*Alexandre Bodard, Zhangsen Chen, Oumayma ELJarray, and Gaixia Zhang**

Green hydrogen (H_2) is an essential component of global plans to reduce carbon emissions from hard-to-abate industries and heavy transport. However, challenges remain in the highly efficient H_2 production from water electrolysis powered by renewable energies. The sluggish oxygen evolution restrains the H_2 production from water splitting. Rational electrocatalyst designs for highly efficient H_2 production and oxygen evolution are pivotal for water electrolysis. With the development of high-performance electrolyzers, the scale-up of H_2 production to an industrial-level related activity can be achieved. This review summarizes recent advances in water electrolysis such as the proton exchange membrane water electrolyzer (PEMWE) and anion exchange membrane water electrolyzer (AEMWE). The critical challenges for PEMWE and AEMWE are the high cost of noble-metal catalysts and their durability, respectively. This review highlights the anode and cathode designs for improving the catalytic performance of electrocatalysts, the electrolyte and membrane engineering for membrane electrode assembly (MEA) optimizations, and stack systems for the most promising electrolyzers in water electrolysis. Besides, the advantages of integrating water electrolyzers, fuel cells (FC), and regenerative fuel cells (RFC) into the hydrogen ecosystem are introduced. Finally, the perspective of electrolyzer designs with superior performance is presented.

1. Introduction

For at least 15 years, the scientific community has agreed that human activities are the cause of global warming, notably due to the quantities of carbon dioxide (CO_2) released into the atmosphere by industry and transport (IPCC reports).[1] To envisage a viable future by 2100, many countries and companies are developing a "net-zero emissions" program for 2050 or beyond.[2] In this quest, hydrogen (H_2), and hydrogen-based fuels are considered key pillars for decarbonization.[3] Combined with efforts to stimulate post-pandemic economic recovery and address inflationary concerns, the global energy crisis has become a major booster for hydrogen-related projects. More than 1.5 billion USD have been invested worldwide in electrolyzer plants, which split water into H_2 and oxygen (O_2, Equation 1) using electricity.[4]

$$H_2O\,(l) \rightarrow H_2\,(g) + \frac{1}{2}O_2\,(g) \qquad (1)$$

Currently, most H_2 is produced from fossil resources (e.g., the steam methane reforming (SMR) method using natural gas), emitting significant amounts of CO_2.[5] Electrolysis is a promising method for producing clean and pure H_2 when the electricity used comes from renewable (e.g., solar, wind, hydro, and tidal energy) or nuclear resources.[6] CO_2 capture is usually applied to reduce CO_2 emissions during H_2 production.[7] The idea of H_2 production from water electrolysis is not new. H_2 was discovered by the chemist Cavendish in 1766. Later in Jules Verne's book The Mysterious Island published in 1875, the fictional character Cyrus Smith refers to water as a future fuel.[6b,8] Other than the potential of being an alternative to fossil fuels, H_2 is overwhelmingly produced as an energy carrier, capable of storing energy and easy to transport.[9] Although some natural reserves of white H_2 (natural H_2, formed by natural processes[10]) have already been discovered, such as the recent discovery in France of a reserve of possibly 46 billion tons of H_2, it is still not sufficient for the modern requires.[11] As outlined in the US National Clean Hydrogen Strategy and Roadmap, green H_2 (produced from renewable electricity), or blue H_2 (produced with few CO_2 emissions), rather than gray H_2 (produced

A. Bodard, O. ELJarray, G. Zhang
Department of Electrical Engineering
École de Technologie Supérieure (ÉTS)
Montreal, Québec H3C 1K3, Canada
E-mail: gaixia.zhang@etsmtl.ca
A. Bodard
IMT Mines Albi
University of Toulouse
Albi 81013, France
Z. Chen
Institut National de la Recherche Scientifique (INRS)
Centre Énergie Matériaux Télécommunications
Varennes, Québec J3X 1P7, Canada

The ORCID identification number(s) for the author(s) of this article can be found under https://doi.org/10.1002/smtd.202400574

DOI: 10.1002/smtd.202400574

Table 1. Advantages and disadvantages of different electrolyzers.

	Advantages	Disadvantages	Refs.
AWE	• Widely commercialized (mature)	• Low current densities	[15b,18]
	• Non-PGM catalyst	• Gas cross-over	[17,18,19]
	• Long-term stability	• Difficile coupling with renewable energies	[15b,18,20]
	• Low cost	• Low reactivity (Cold start to nominal load < 50 min, Hot start in minutes, Shutdown in minutes)	[15b,18a, 20]
	• MW range	• Low operating pressure	[15b, 17, 18, 19a, 20a, 21]
		• Corrosive liquid electrolyte (20%–30% KOH)	[17, 18b]
PEMWE	• Commercialized	• High-cost components (noble metal Pt, Ru, Ir)	[18a]
	• High load range	• Corrosive environment	[15b, 17, 20a, 22]
	• Compact cell design		[18a]
	• High operating pressure		[15b, 18a, 20a, 22]
	• High H_2 purity (99.9%–99.9999%).		[15b]
	• Coupling with renewable energies is achievable		[15b]
	• High reactivity (Cold start to nominal load < 20 min, Hot start in seconds, Shutdown in seconds)		[15b, 18a, 20b]
	• High current densities		[15b, 18b, 22]
	• Higher voltage efficiency		[19a]
AEMWE	• Non-noble metal catalyst	• Early commercialization stage	[2, 5b, 18a]
	• Less corrosive electrolyte	• Membrane stability	[15b, 18]
	• Compact cell design	• Low durability	[17, 18, 19a]
	• High operating pressure		[15b]
	• Coupling with renewable energies is achievable		[15b]
	• High current densities		[23]
	• High reactivity (Cold start to nominal load < 20 min)		[15b]
SOEC	• High efficiency	• Early commercialization stage	[1, 2, 15b, 20a, 21]
	• Non-noble catalyst	• Large system design	[18a]
		• Low durability	[15b, 18a, 20a]
		• Need proximity to a heat source (Operating temperature 700–850 °C)	[15b]
		• Low reactivity (Cold start to nominal load > 600 min, Hot start in minutes)	[15b, 18a]
		• Low current densities	[2]
		• High cost	[15b, 18a, 20a]

from natural gas reforming) must first be used in the hard-to-decarbonize areas, such as the industrial sector (e.g., chemicals, steel, and refining) and the heavy-duty transportation.[12] Given the power difference between hydrogen refueling stations (HRS, megawatt (MW) range) and industrial installations (10 MW range), developing HRS becomes a priority to gain feedback before embarking on industrial projects. Then, green and blue H_2 can be used for long-term energy storage to enable a clean grid.[13] With the power-to-gas concept in the clean grid, renewable energy generation can exceed 100% of demand (it happened in Spain on Tuesday, May 16, 2023, for nine hours).[14] Under this circumstance, it will mostly be more efficient to export this surplus to neighboring countries than to convert it back into H_2 due to the energy loss concerns.[15] In all, H_2 and renewable energy-generated electricity are essential to the decarbonized society. The former enables energy storage through the "power-to-gas" concept. The latter enables low electricity prices, which represent the main cost of electrolysis.[15b]

To produce green H_2, several electrolysis systems are in the spotlight, such as those operating at low temperatures, the alkaline electrolyte (i.e., alkaline water electrolysis, AWE) or solid electrolyte (i.e., anion exchange membrane water electrolysis, AEMWE), the acid one with solid electrolyte (i.e., proton exchange membrane water electrolysis, PEMWE), and the one operating at high temperatures (i.e., solid oxide electrolysis cell, SOEC). Their advantages and disadvantages are discussed in **Table 1**. AWE is in the MW range and has a long durability. However, it is already mature with liquid electrolytes, making its system design renovation particularly difficult. Therefore, AWE has fewer prospects for evolution than other solid membrane electrolyzers (i.e., PEM, AEM, and SOEC). Although SOEC electrolyzers may be more efficient than low-temperature

electrolyzers, they will not be discussed in this study as they operate at high temperatures, making them dependent on heat sources. A solid membrane electrolyte makes it possible for the electrolyzers to work under high pressure, eliminating the need for a hydrogen compressor in the system.[16] The PEMWE and AEMWE systems are the most promising electrolyzers since they can also produce H_2 directly under pressure, thus promoting the use of H_2 as an energy carrier and storage system.[17] Moreover, their high reactivity makes them particularly suitable for coupling with renewable energies to potentially achieve decarbonized industrialization.

This scientific review aims to provide a comprehensive analysis of the state-of-the-art technologies and advancements in electrolysis focusing on PEM and AEM electrolyzers, their challenges, and perspectives. Fuel cells and regenerative fuel cells will also be discussed, as they are part of the evolution of electrolyzers due to their functional proximity and the need for a clean grid. In addition, the global hydrogen ecosystem aiming toward a decarbonized society is briefly introduced and discussed.

2. Low-Temperature Electrolyzers with Solid Membrane

2.1. Hydrogen Evolution Reaction and Oxygen Evolution Reaction

The electrolysis of water, represented by Equation 1, involves two distinct half-cell reactions known as the hydrogen evolution reaction (HER) and the oxygen evolution reaction (OER). In a typical acid-electrolyte water electrolysis, H_2O is oxidized at the anode to produce O_2 (Equation 2) while H^+ is reduced at the cathode to generate H_2 (Equation 3). Electrochemical production of H_2 from water requires an input of energy to overcome the inherent barrier, referred to as the overpotential (η). The overpotential is defined as the difference between the potential (voltage) $E(i)$ of a specific half-reaction (0 V vs. reversible hydrogen electrode (RHE) and 1.23 V vs. RHE for HER and OER, respectively, as determined by thermodynamics) and the experimental potential E_0 at which the redox reaction is observed. The thermodynamic voltage of a water electrolyzer is 1.23 V. The larger the overpotentials of HER and OER of the electrocatalysts, the higher the cell voltage values the water electrolyzer will have. Based on the Nernst equation, OER prefers alkaline conditions while HER is favored in acidic media.[24]

In both the HER and OER systems, the efficient production of H_2 and O_2 relies on the presence of suitable electrocatalysts that minimize overpotentials. These catalysts play a crucial role in reducing the energy input required for the electrochemical reactions, leading to more efficient and sustainable production of H_2 and O_2.[25] Noble-metal-based catalysts are preferred in acid electrolyte water electrolysis for their robust nature to the corrosive environment. To reduce the cost of catalyst fabrication, alkaline electrolyte water electrolysis broadens the catalyst options to transition-metal-based catalysts. Noble metals like Pt,[26] Ir,[27] Ru,[28] are commonly studied in water electrolysis because of their promising overall performance in acid electrolytes and sometimes in alkaline electrolytes (mostly Pt-based for HER, Ir- and Ru-based for OER). For non-noble metals, Mo-based catalysts show great potential for HER,[29] Co-based and Ni-based catalysts are good for OER[30] and HER.[31] Transition-metal-based alloy catalysts recently demonstrated superior catalytic performance to conventional catalysts, including Ni/Fe-based,[29,32] Co/Fe-based,[33] and Ni/Cu/Mo-based[34] electrocatalysts. Intriguingly, some of these promising non-noble-metal-based materials can serve as bifunctional catalysts (i.e., active for both HER and OER) that could be employed in a symmetric cell to simplify the electrolyzer setup. The details of the corresponding electrocatalysts will be discussed in the following sections of this review.

2.2. Proton Exchange Membrane Water Electrolyzers (PEMWE)

Figure 1a depicts a 3D diagram of a real PEMWE cell. The operating principle of the PEMWE is to pump pure water to the anode port, which flows through the bipolar plates (BPs) and gas diffusion layers (GDLs) to the surface of the anode catalyst, where it is dissociated into protons (H^+), O_2, and electrons (e^-). The O_2 is released into the water stream, while the protons pass through the solid polymer electrolyte (SPE), under the effect of the concentration gradient and the electric field, to the surface of the cathode catalyst to immediately recombine with the electrons to form H_2. The electrons in the external electrical circuit are released at the anode to generate the direct current (DC). They provide the driving force (cell voltage) for the reaction.[21,36] The main component of a PEMWE is the membrane electrode assembly (MEA) composed of the SPE sandwiched between the two electrodes and the BPs. The electrodes are composed of a porous catalyst layer (CL) and even more porous GDLs (Figure 1b). These are finally encased by the end plates which provide mechanical support and serve as fasteners for all components. The CL contains evenly dispersed electrocatalysts on a nanoporous support. It allows the reduction of the activation energy and promotes charge transfer kinetics. The GDLs, sometimes called the porous transport layer (PTL), play the role of the current collector. The addition of metallic meshes or sinters in GDLs can improve the charge transfer. BPs are primarily responsible for the uniform distribution of water in the cell. In addition, BPs function in heat transfer, separation of anode and cathode compartments, and conductivity.[36a,37] The efficiency of the PEM electrolyzer, particularly at higher current densities, is highly dependent on the contact and interface structure between these multiple components.[21,36a] As highlighted before, the electrocatalysts on both the anode and the cathode are essential and represent one of the main challenges of PEMWE.

2.2.1. Anode Engineering

The OER (Equation 2) takes place at the anode, which occurs simultaneously with the HER (Equation 3) of the cathode.

$$2H_2O\,(l) \rightarrow 4e^- + 4H^+\,(aq) + O_2\,(g) \quad (2)$$

$$2H^+\,(aq) + 2e^- \rightarrow H_2\,(g) \quad (3)$$

Unfortunately, because of the multiple proton and electron transfer, the OER has sluggish kinetics. It translates to a larger

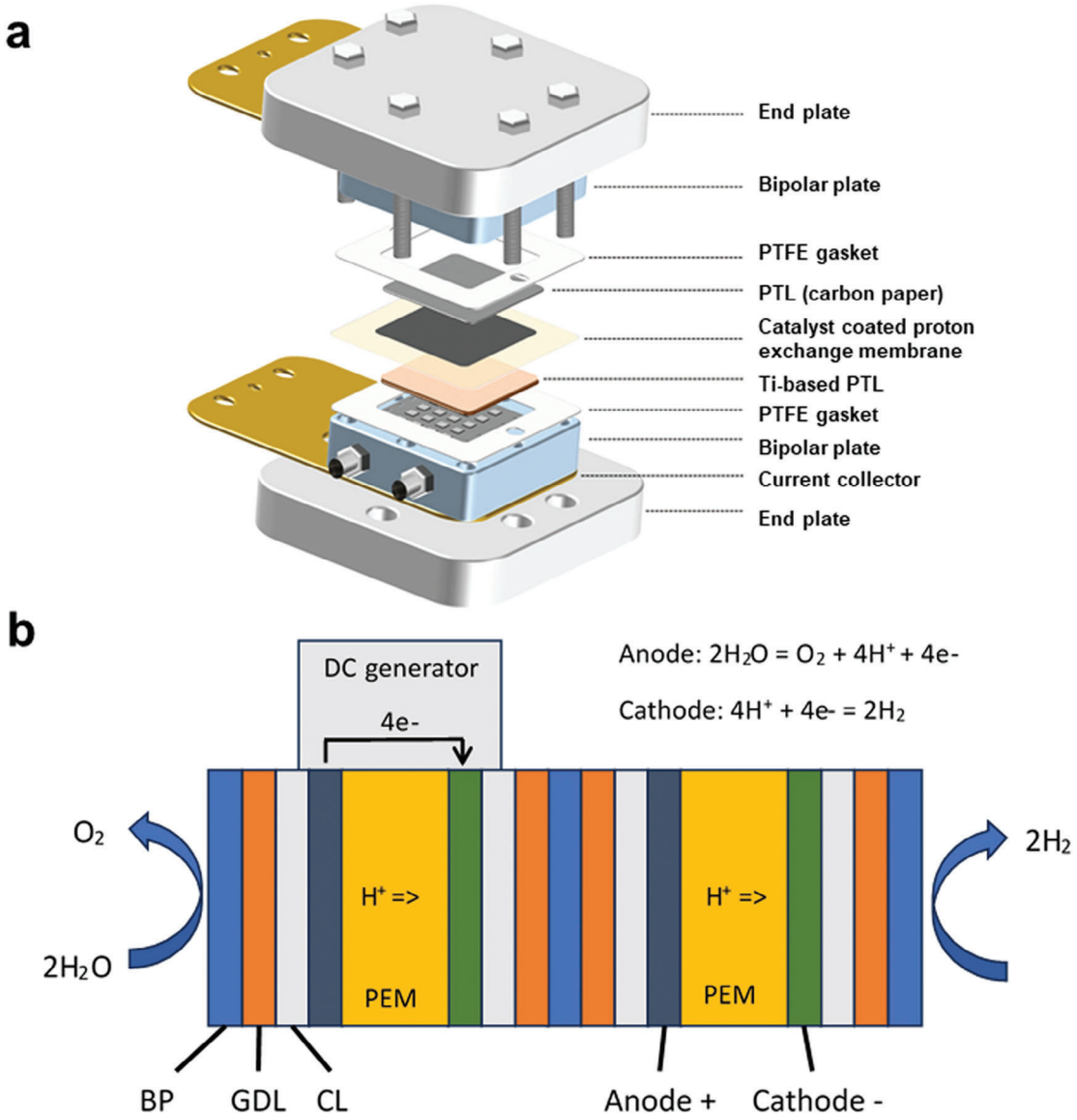

Figure 1. a) The 3D diagram of a PEM cell. Reproduced under terms of the CC-BY-NC-ND 4.0 license.[35] Copyright 2021, Chang Liu et al., published by American Chemical Society, no change was made, https://pubs.acs.org/doi/10.1021/acsami.0c20690. b) PEMWE two cells representation extracted from a stack.

anodic overpotential (η_a) than cathodic overpotential (η_c), making OER one of the main problems that hold back the commercialization of PEMWE.[38] Apart from water electrolysis, OER is commonly the half-reaction in many electrocatalytic systems such as regenerative fuel cells, CO_2 reduction, metal-air batteries, and nitrogen fixation. It urges the studies to improve OER activity for electrocatalysis.[39] Water dissociation produces a huge quantity of protons, leaving the reaction environment acidic. It requires the OER catalyst to be stable in an acidic environment. There are two main mechanisms for the OER in an acidic environment: the adsorbate evolution (AE) mechanism and the lattice oxygen-mediated (LO) mechanism.[40] Wu et al. concluded that LO-dominated catalysts are more active but less stable than AE-dominated catalysts.[36a] Although a balance between activity and stability is required, stability matters first for the catalyst in the PEMWE application. External factors such as catalyst detachment and surface blocking, as well as internal factors such as catalyst dissolution and surface reconstruction, are primary reasons for catalyst instability and deactivation. Among them, dissolution is the main parameter affecting the stability of OER electrocatalysts.[40] Consequently, to obtain a highly stable catalyst, dissolution must be inhibited. The interaction between the different dissolution and deposition pathways is governed by the kinetics of the associated reactions. To fully understand the complex relationship between catalyst activity and stability, further exploration is required through advanced kinetic simulations and characterization techniques in real catalytic systems.[36a]

Common Iridium (Ir), Ruthenium (Ru), and Non-Noble Metal-Based Anode Catalysts: Currently, research is being carried out mainly on three types of anode catalysts: Ir-based, and Ru-based,

due to their high metallic conductivity of 10^4 cm^{-1} ohm^{-1},[21] and noble metal-free anode catalysts. The "volcano plot" calculated using density functional theory (DFT) suggests that noble metals generally have appropriate intermediate adsorption free energies, leading to better OER activity than that of non-noble metals. Besides higher activity, noble metal catalysts also exhibit better stability compared to non-noble metal catalysts. Theoretically, the d-electron orbitals of the noble metal electrocatalysts (e.g., Ir and Ru) are unfilled. It is easy for reactants to be adsorbed on the catalyst surface with moderate adsorption energy, favoring the formation of reactive intermediate and contributing to the high catalytic activity. Thus, Ir/Ru-based metal/oxide materials dominate the acidic OER in commercial PEMWE devices for their unique catalytic properties.[41] IrO_2, with a loading of 2–2.5 mg cm^{-2}, is the most used anode catalyst in PEMWEs, thanks to its stability.[36a,42] Due to its high cost and insufficient activity, solutions containing less iridium but with better activity are being sought. Regulating the structure of Ir metal is a way to improve activity and durability while reducing the Ir load on the OER. The Ir metal irreversibly oxidizes to Ir oxide during the catalytic reaction. Low-crystallinity Ir oxide, namely IrO_x, tends to show better OER activity than that of IrO_2. However, the low structural stability of IrO_x because of the Ir dissolution during the catalytic process reduces the lifetime of PEMWE. Yu et al. dispersed IrO_x in the Nafion catalyst layer to solve this dissolution problem. The IrO_x/Nafion catalyst uses an Ir loading of ≈0.08 mg cm^{-2} (≈1/30th the commercial Ir loading in PEMWE) and shows good activity (current density of 1.8 A cm^{-2}) and stability (4500 h under PEMWE operation).[43] Another way of reducing the iridium loading is to introduce less expensive components with higher activity than those of IrO_2, such as RuO_2 (which has lower stability but higher activity than those of IrO_2).[36a,37,39] This strategy has proved effective in numerous studies. For example, Du et al. placed Ru atoms in an IrO_2 matrix, allowing the Ru-IrO_2 matrix to be dominated by LO,[44] which enhances its activity (current density of 1 A cm^{-2} at a cell voltage of 1.722 V in PEMWE, better than 1.820 V of the conventional IrO_2 anode catalyst). With the same idea, doping of non-noble metal can further reduce the overall cost of the catalyst fabrication. Unfortunately, a minimum of 50 wt.% of Ir is needed in the anode catalyst to keep a good OER activity, which is still too much.[36a] Another idea is to disperse Ir or IrO_2 on non-noble metal oxide supports such as TiO_2. However, the low conductivity of metal oxides leads to a high Ir load.[45] Kim et al. overcame this conductivity issue by choosing TiO_2-MoO_x composite as support. The development of Ir-based supported anode catalysts can not only reduce the use of Ir but also balance the activity-stability relationship of anode catalysts.[46] Iridates, which are oxides containing Ir and one or more metallic elements, show promise as low-Ir loading OER anode catalysts. Iridates exhibit good OER activity and stability thanks to their crystalline structures.[36a] As for Ru-based anode catalysts, their low stability hinders their future achievement in the performance required for industrial PEMWEs. Although some strategies (e.g., elemental doping) are being investigated to improve their stability, Ru-based catalysts can currently only be used in combination with Ir-based anode catalysts. Non-noble metal anode catalysts present the same problem as Ru-based anode catalysts in terms of stability, but they also exhibit low activity which makes them not comparable to commercial materials.[36a,39] Acid stability remains a major challenge for OER electrocatalysts in industrial applications.[39] Indeed, OER performs better in an alkaline environment, while HER operates more successfully in an acidic environment.[25]

2.2.2. Cathode Engineering

Popular Platinum-Group Metal (PGM)-Based Catalysts for Cathode: In current PEMWEs, noble metal-based electrolysts, such as the IrO_2/RuO_2 catalysts for the OER and platinum (Pt)/palladium (Pd) catalysts as the cathode for the HER, are commonly applied. PGM-based catalysts and their derivatives are recognized as highly efficient catalysts for the HER. This is attributed to their favorable properties such as excellent stability and HER activity in acidic environments. According to the Sabatier principle, due to their optimal hydrogen binding energy (HBE) and Gibbs free energy for atomic hydrogen adsorption (ΔG_{H^*}), low activation energies are required for hydrogen desorption from the surface of PGM-based materials.[47] It renders PGM-based catalysts the ability to achieve a high exchange current density near the thermodynamic potential. These catalysts also exhibit a small Tafel slope and deliver close to 100% Faradaic efficiency. Despite their exceptional performance, the widespread application of PGM-based catalysts for large-scale H_2 production is hindered by the high cost and limited reserves of precious PGMs on Earth. Therefore, it is imperative to address these challenges by reducing the noble metal loading and potentially replacing them entirely with earth-abundant and non-noble metal alternatives that offer high catalytic activity and stability.[25]

Numerous noble metals, non-noble metals, and metal-free nanoparticles HER electrocatalysts are currently being studied. First, the noble metal-based catalysts with the most efficient Pt followed by Pb and Ru. Pd and Ru-based catalysts are studied to compete for their efficiency to that of the Pt-based catalysts. Pd shows a similar atomic size to Pt[25] and is three times more abundant in the earth's crust.[48] As for Ru, it is two times cheaper than Pt according to the June 13, 2023, cost update,[49] and displays a moderate Ru−H bond strength like Pt.[25] Unfortunately, Pd and Ru also have their own issues. Pd has become more expensive than Pt since 2019.[50] Ru is five times less abundant on the earth curst than Pt.[48] This justifies that even the other noble metals will not replace Pt without a proper solution to reduce noble metals load on HER catalysts while keeping high stability and activity. Nanoparticle engineering strategies are promising in this quest as the adjustments in size, shape, crystallinity, facet, etc. of the electrocatalysts play key roles in HER activity. One way to improve the specific area of the catalyst is by creating porous structures.[25] There are several other improvements in catalyst engineering, such as the use of support materials or single-atom catalysts, which offer high stability and activity with minimal Pt loading. To reduce the amount of Pt required, the implementation of supported single-atom catalysts has shown promise in maximizing the efficiency of Pt use. This is achieved by dispersing the highly active Pt in the form of the supported single-atom moiety on the substrate, ensuring maximum and optimal utilization of the Pt component.[25,39,51] Apart from structural engineering, compositional engineering by alloying Pt, Pd, or Ru with less expensive metals can also enhance the catalytic

performance of the electrocatalysts.[6b] This approach is constantly improving, as shown by the recent study of our group. A simple and easy-to-implement molten salt-assisted strategy (**Figure 2**a) was developed for the synthesis of a series of noble metal-based carbon group intermetallic compounds, such as PtSi (Figure 2b–d), at moderate temperatures and ambient pressure. This synthetic strategy is universal and facile, which can be employed on many noble metals such as silicides: PtSi, Ru_2Si_3, and RhSi; stannide: RuSn; and germanide: Ru_2Ge_3. The as-prepared PtSi exhibits high HER activity and stability over a wide pH range (0–14), which covers the acid, neutral, and alkaline media, as shown in Figure 2e–g. Its activity is comparable to that of the state-of-the-art Pt catalyst. To better understand the intrinsic activity of PtSi in HER, DFT calculation was involved (Figure 2h). The projected density of states (PDOS) in Figure 2j demonstrates the electronic states crossing the Fermi level, implying conductive behavior. The down-shift of the D-band implies a lower desorption between adsorbed H species and PtSi, which favors HER. The choice of Si is justified by its ability to reduce the hydrogen bonding energy on the Pt surface (Figure 2i) and by its high availability as the second most abundant element on earth.[52] This alloy PtSi strategy significantly reduces the cost of noble-metal catalyst fabrication while providing efficient catalytic activity in a wide pH range, which holds great promise in scale-up production of low noble-metal loading HER catalysts.

Although many improvements are being made to reduce the noble metal loading in HER catalysts, the simplicity and ease of scaling up the process also require attention. Indeed, most synthetic processes are complex and expensive, resulting in high production costs for the final catalytic products. Furthermore, the yields and quality of these catalysts are insufficient to meet the demands of industrial and commercial applications.[25] The same conclusions go for non-noble-transition-metal. Their performances have been significantly improved for HER, but it is still not enough. Performances of most non-noble-transition-metal catalysts are not comparable to those of Pt-based catalysts in terms of stability, activity, and durability in a wide pH range. The few that do are mainly Mo- and W-based ones. In addition, there is a need to improve the understanding of the HER mechanism for transition metals, as most current interpretations are based on the classical theory of noble metal catalysts.[25] To achieve this, in situ characterization needs to be developed not only for non-noble metals but also for all HER catalysts, which are currently limited to ex-situ characterization (i.e., before and after HER). Ex-situ characterizations fail to capture crucial information, including the identification of reaction intermediates adsorbed on the catalyst surface, the evolution of active sites, a and the structure of the catalysts during the HER process.[25,39,53] The search for metal-free HER catalysts is mainly carried out on graphene and g-C_3N_4, trying to improve their activity by adjusting their electronic structures thanks to non-metallic elements doping.[25]

A major problem currently highlighted in the literature is the lack of a standard to compare different catalysts. It leads to too many papers claiming to have synthesized an electrocatalyst with higher stability and activity than those of the commercial one. However, they are rarely tested under the same conditions.[25,36a,37,39–40,54] Laboratory tests are often done in half-cell set-up with three electrodes (**Figure 3**a[36a]) but it does not take into consideration the mass transfer loss and ohmic resistance of the catalysts layer[36a,55] (Figure 3b). Besides, laboratory experiments also overestimate the stability of the MEA at least on the anode side.[56] An efficient and safe production of hydrogen also relies on the membrane performance.

2.2.3. Electrolyte/Membrane Engineering

Nafion-Based Membrane Designs: The most commonly used membrane in PEMWE is Nafion® (a registered trademark of DuPont). The thin polymer membrane of Nafion ensures a compact cell design, high proton conductivity, and excellent mechanical stability in an acidic environment, thanks to the presence of sulfonic functional groups (R-SO_3H).[37] These groups are responsible for the proton conductivity via an ion exchange mechanism (vehicle and hopping mechanism), as represented in **Figure 4**a,b.[57,58] Nafion also has the advantage of low gas crossover, enabling the production of highly pure hydrogen. However, this low gas crossover performance diminishes with the increases in pressure and temperature, necessitating a robust PEM for practical and safety applications.[59] The presence of H_2 with O_2 (especially the high H_2 in O_2 content in the anodic compartment) may lead to an explosion,[60] or even before the explosion, to the generation of heat which will damage the system.[55] Unfortunately, simply applying a thicker membrane reduces overall catalytic efficiency.[15b,61] To avoid the H_2 crossover issue, several propositions have been made. A Nafion/graphene/Nafion PEM, studied by Bukola et al., exhibits high proton conductivity and eight times lower H_2 crossover (2.6×10^{-9} mole cm^{-2} s^{-1} and 3×10^{-8} mole cm^{-2} s^{-1} for the Nafion/graphene/Nafion membrane and Nafion 211 membrane, respectively) thanks to the graphene properties.[62] Other studies applied Pt nanoparticles as an interlayer between the electrodes to recombine hydrogen with oxygen, decreasing the H_2 in O_2 content at the anodic compartment in PEMWE.[63]

For the stability issue, the Nafion polymer electrolyte is one of the components responsible for the degradation of the PEMWE during long-term operation.[64] Both the electrolysis unit components and the cationic impurities released by the feed water into the cathode cell will occupy the ion exchange sites of the Nafion in the catalyst layers and membrane.[65] With noble metal electrocatalysts usually being applied in PEMWE, its high cost drives the search for inexpensive alternatives.[16,18b,66]

An alternative to Nafion, studied by Park et al. the sulfonated poly(arylene ether sulfone) with a degree of sulfonation of 50 mol.% (SPAES50) shows high performance without H_2 crossover and at a lower price. The SPAES50 membrane with 20 µm used in PEMWE achieves 1069 mA cm^{-2} at 1.6 V and therefore surpasses Nafion-based PEMWE and other perfluorosulfonic acid and hydrocarbon membranes.[67] Another disadvantage of the Nafion membrane is its sensitivity to dehydration, which causes a decrease in proton conductivity under boiling water temperature conditions.[68] Working at high temperatures has the advantage of increasing the electrode kinetics. To take this opportunity, TiO_2 and SiO_2 have been incorporated into the Nafion membrane for their water retention properties, enabling these membranes to operate above the boiling temperature of the

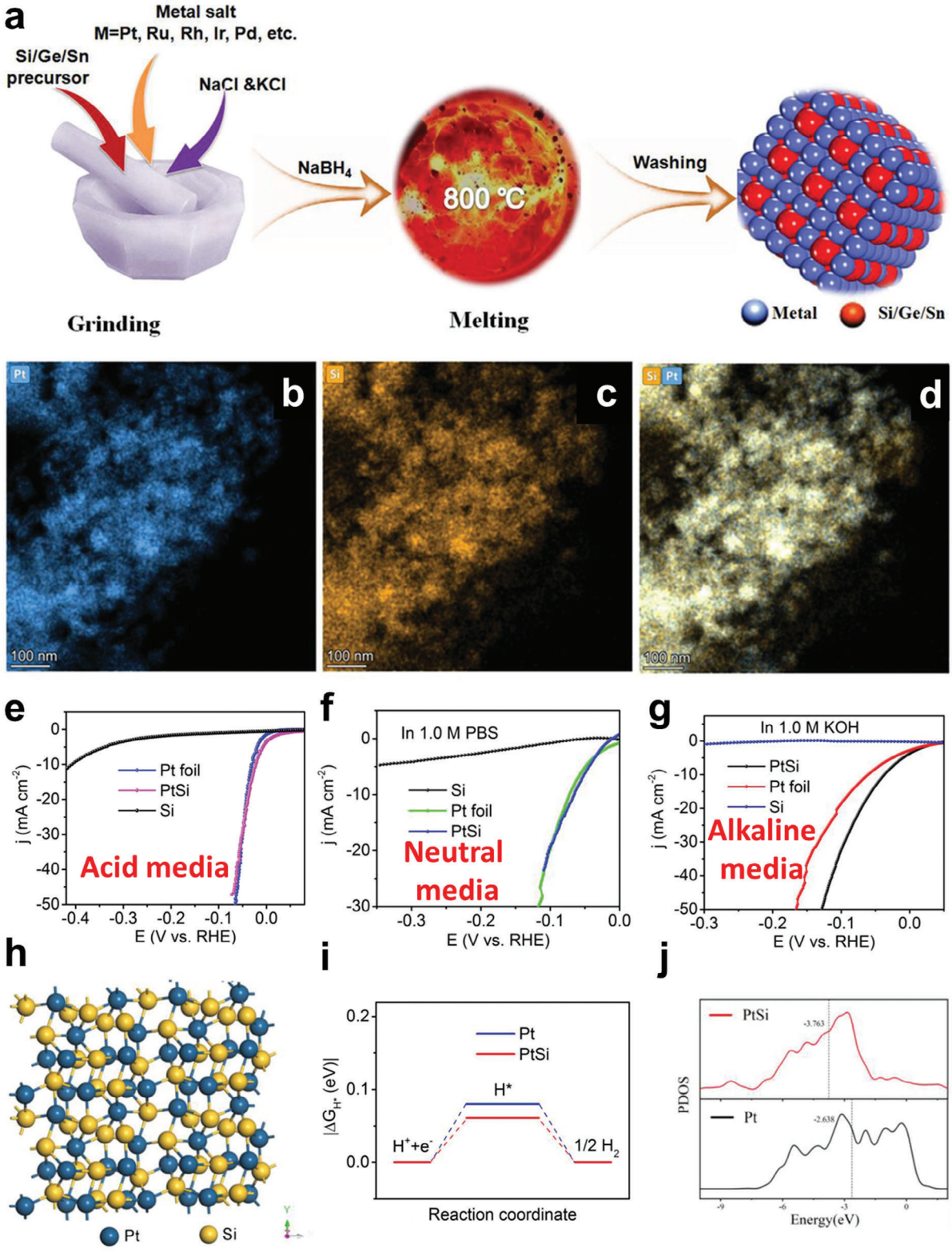

Figure 2. a) The schematic diagram of the molten salt-assisted strategy for noble metal-based carbon group intermetallic compounds. The STEM-EDS elemental mapping images of as-prepared PtSi: b) Pt, c) Si, and d) Pt + Si. The HER polarization plots at a scan rate of 5 mV s^{-1} for Si, Pt foil, and PtSi in the electrolyte of e) 0.5 m H_2SO_4, f) neutral, and g) alkaline solutions. h) DFT model for PtSi. i) The HER free-energy calculations at equilibrium potential for Pt and PtSi. j) The d-orbital PDOS of PtSi and Pt. Reproduced with permission.[52] Copyright 2022, Wiley-VCH GmbH.

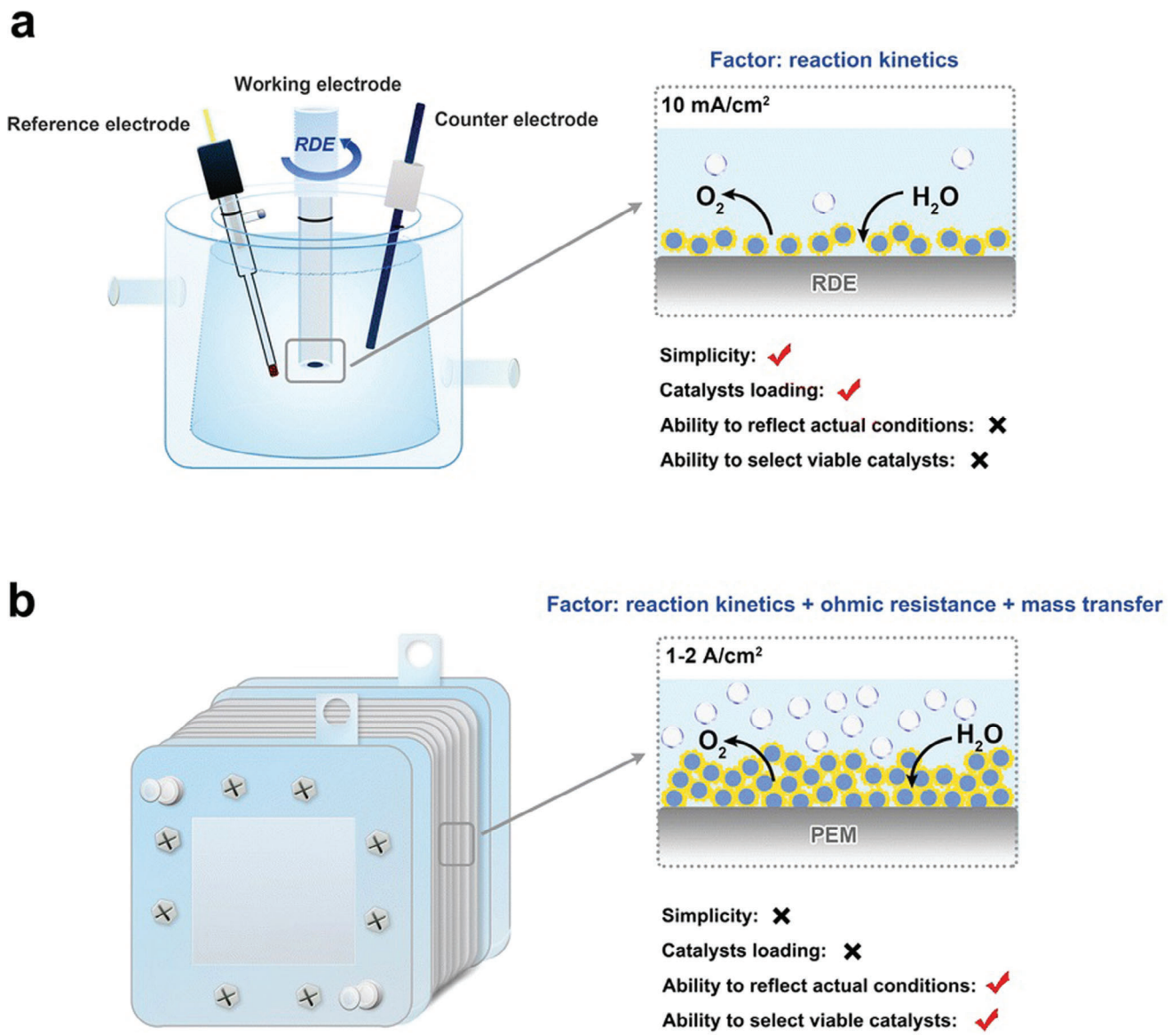

Figure 3. a) Left: the three-electrode HER cell schematic. Right: the enlarged illustration of CL on a rotating disk electrode (RDE) and the pros and cons of the three-electrode HER cell. b) Left: the PEM electrolyzer schematic. Right: The enlarged illustration of CL on MEA and the pros and cons of PEM electrolyzer. Reproduced with permission.[36a] Copyright 2023, Royal Society of Chemistry.

water.[69] It should be noted that Nafion-TiO_2 has only been tested for PEMFC in the literature. To achieve a high-performance electrolyzer, it is crucial to perfectly combine the above-mentioned materials in a single system.

2.2.4. Cell Assembly Engineering

Bipolar Plates: For industrial water electrolysis, the price of electricity is the most expensive part during operation (e.g., for a 1MW PEMWE).[19] After the power supply, it is the bipolar plates (BPs) that cost the most in the PEMWE stack with a medium potential for cost reduction according to IRENA.[15b] BPs are electrically-conducting plates that are essential to join together the cathode and the anode of the cells. The BPs are currently composed of graphite, nickel, or stainless steel (SS) due to cost concerns.[70] On the anode side of PEMWE, the corrosive and oxidative operating environment restricts materials to robust titanium (Ti) bases for GDL and BPs.[55,71] However, the long-term operation of water electrolyzers in humid and acidic conditions inevitably results in the degradation and the corrosion of metal-based BPs. The mitigation of this issue can be realized by applying protective coatings on BPs to safeguard the surface, as summarized by Choi et al.[72] To find a cost-efficient alternative for BPs, low-cost metal-coated Ti alloy seems to be a necessity. A recent article[71] improves the performance of Ti BP by a cathode plasma electrolytic deposition of nitrogen-chromium composite. The BPs with TiN/CrN composite coating obtained

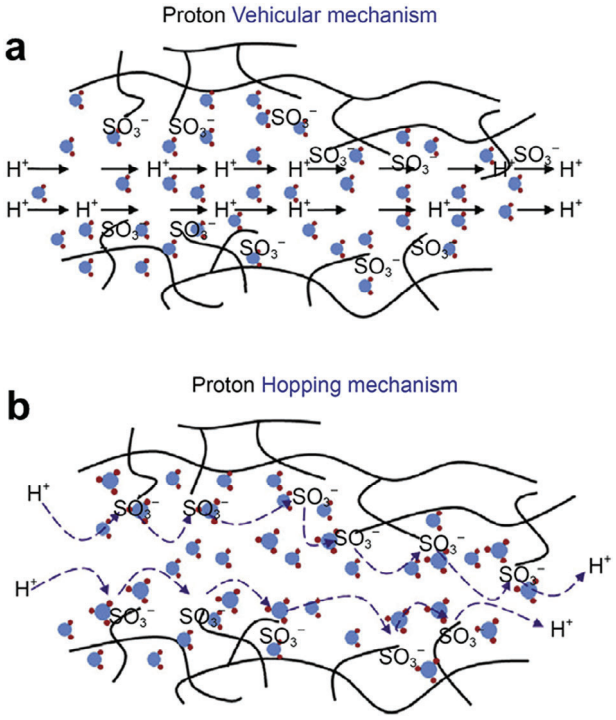

Figure 4. The schematics of a) The Vehicular mechanism and b) The hopping mechanism of the proton conduction in a Nafion membrane. Reproduced under terms of the CC BY-NC-ND 4.0 license.[57] Copyright 2022, Li-Yu Zhu et al., published by Elsevier B.V., no change was made, https://www.sciencedirect.com/science/article/pii/S1995822621001382#fig3.

considerable corrosion resistance and good conductivity in an anode environment in PEMWE. Despite the developments in corrosion-resistant metal BPs, carbon-based BPs are still of interest for their inexpensive nature. Messing et al. analyzed the uncoated carbon BPs (C-BPs) as the alternative to Ti BPs.[73] It turns out that C-BPs applied in PEMWE exhibited low degradation rates (31.92 μV h^{-1} at 3 A cm^{-2} and 16.41 μV h^{-1} at 1 A cm^{-2}), which were lower than those of Ti-BPs. It highlights the potential of the application of C-BPs in water electrolyzers, which will greatly contribute to reducing the cost of the cell setup. Another recent article studied the different PTLs for PEMWE.[74]

Practical Genres of Membrane Electrode Assembly: Another impactor on the efficiency of the stack is the MEA fabrication process. There are two main ways to prepare membrane electrode assembly (MEA), the catalyst-coated substrates (CCSs) method (also named catalysts coated on gas diffusion layer (CCG) or porous transport electrode configuration (PTE, **Figure 5**b)[75]) and the catalyst coated on the membrane (CCM) method (Figure 5a). CCM is to either deposit the catalyst directly on the membrane or transfer the catalyst on the membrane through a decal process. It requires a pre-manufactured, freestanding membrane to proceed with CCM.[76] PTE is to deposit catalyst directly on the porous transport layers, as depicted in Figure 5e. The self-supported electrode is another popular type of PTE.[75] For PEMWE, the MEA is commonly prepared with the CCM method where CCM is located in the middle of the cell composed of a cathode CL, a PEM, and an anode CL (Figure 5d) as it shows better performance.[55,77] However, the operation conditions of PEMWE need to be taken into consideration when applying the MEA fabrication methods. Bühler et al. found that the performance of the PTE method became better than that of CCM when the PEWME operates above the current density of 750 mA cm^{-2}.[78] A new method, direct membrane deposition (DMD, Figure 5c), also attracts attention as the membrane is directly fabricated on the gas diffusion electrode in the DMD method (Figure 5f). It facilitates the incorporation of nanostructured catalysts (e.g., nanoparticles and nanofibers) in MEA. DMD provides enhanced electrochemical performance while reducing catalyst loading. It can reduce the noble metal loadings in PEMWE, thus decreasing the overall cost of the device.[76,79]

Electrolyzer Stack Prospects: There is a significant lack of publications on global analyses of the PEMWE stack. The related research articles were mainly published around 2010. Recent stack-concerning research mainly speaks of fuel cells or cost comparison. One way of reducing the cost of PEMWE is to work at high pressure, which would eliminate the need for energy-intensive compressors.[80] However, as pointed out above, the high-pressure operation requires solid components, which are therefore more expensive than ambient ones. A balance has to be found between component cost and high pressure. Another advantage of the PEMWE stack over the AWE stack is that the equipment around the PEMWE (e.g., dryer, compressor, gas separator, etc.) is much simpler than those around AWE.[15b]

A recent study highlights the fact that in 2021, not a single PEMWE cell had achieved the performance for widespread application. This performance is a cell activity over 1.0 A cm^{-2}, an Ir-power density over 50 kW/g_{Ir} at 1.6 V, and a degradation rate under 6 μV h^{-1}.[81] It is important to keep trying to improve the performance of PEMWE cells. Another way of improving the performance and reducing costs is to replace PEMWE with AEMWE, which requires non-noble metals.

2.3. Anion Exchange Membrane Water Electrolyzers

The operating principle of the anion exchange membrane water electrolyzer (AEMWE) is similar but with some differences to that of PEMWE. Their main similarities are the presence of a solid membrane, CLs, BPs, GDLs, the same reactant (i.e., H_2O), and products (i.e., H_2 and O_2). The reactions at the anode and cathode are different from those in PEMWE since the environment is alkaline. It is not H^+ that is carried from the anode to the cathode but OH^- from the cathode to the anode (**Figure 6**a,b). The water flow is directed toward the cathode port to be dissociated into H_2 and OH^-. The H_2 is released at the cathode while the OH^- passes through the AEM and forms H_2O and O_2 at the anode. To increase AEMWE performance, it is common to add a flow of dilute alkaline solution in the cell for most studies.[18b,54,70,83a,84] To enhance the performance in the electrode-electrolyte interface, the ionomer is sometimes added to the AEMWE. It also plays the role of uniformly distributing the catalysts which ensures the exchange of ions between the catalyst surface and the membrane via its functional groups, improving the performance in the 3-phase boundary (gas, liquid, and solid).[85] The AEMWE is promising as it has the advantages of both PEMWE and AWE.[54,86] However, it still faces many issues and requires more research on its components since AEMWE mainly inherits

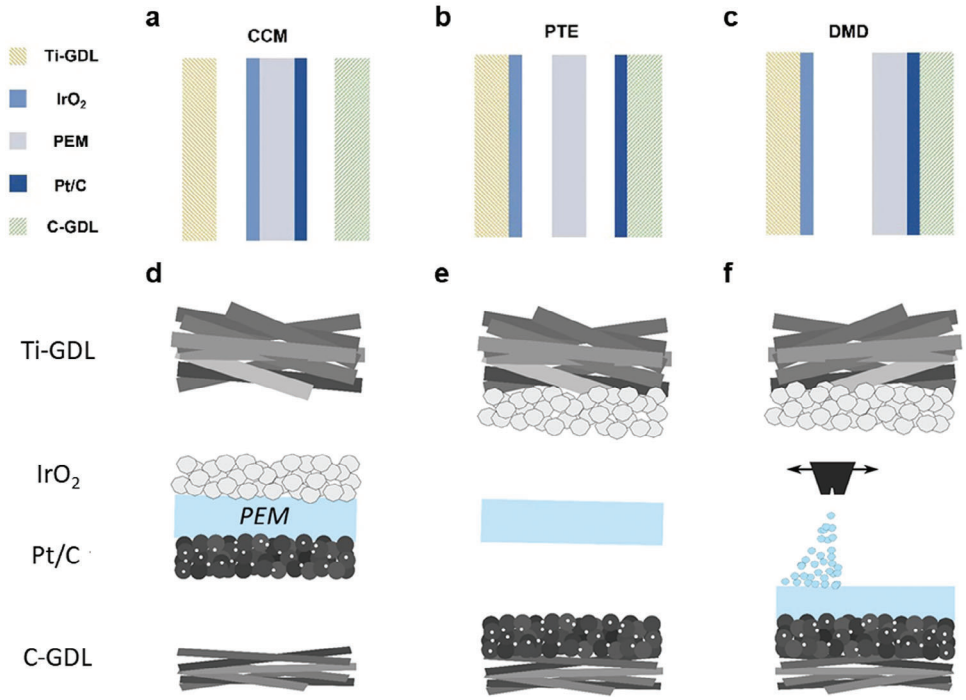

Figure 5. Three mostly studied MEA components of PEMWE and their schematic illustrations of a) and d) CCM; b) and e) PTE; and c) and (f) DMD. a–c) Reproduced under terms of CC BY 4.0 license.[55] Copyright 2022, Kexin Zhang et al., Published by Tsinghua University Press. d–f) Reproduced under terms of CC BY 4.0 license.[76] Copyright 2019, Peter Holzapfel et al., Published by Elsevier B.V.

materials from AWE and PEMWE, resulting in poor stability and durability.[54] The best performance of AEMWE currently comes from PEMWE materials with noble metals. AEMWE research therefore aims to find materials specially adapted to AEMWE. Catalyst research needs to focus on non-noble metals, as they represent one of the key cost-saving advantages of AEMWE.

2.3.1. Anode Engineering

As highlighted before, due to the overpotential at the anode and cathode, they both require highly efficient electrocatalysts, especially the anode one since the OER overpotential is significantly higher than that of HER. Efficient electrocatalysts not only reduce the overpotentials but also improve the overall cell life.[84a] Compared to PEMWE, AEMWE does not have an acidic environment and thus can work more easily with non-noble metal. Currently, IrO_x (with different nanostructures, **Figure 7a–c**)[87] is widely used as an anode electrocatalyst for AEMWE.

NiFe-Layered Double Hydroxides (LDH) Anode Catalysts: Adapting the nanostructure concept, Koshikawa et al. synthesized a single nanometer-sized NiFe-LDH (Figure 7d) as an electrocatalyst for the anode, known as one of the best non-noble catalysts so far in AEMWE.[88] This catalyst possesses better OER activity than IrO_x in both half and single cells with a lower overpotential (Figure 7e, overpotentials of 247 and 281 mV for NiFe-LDH and IrO_x, respectively) to reach 10 mA cm^{-2}. In an AEMWE full cell with 1 M KOH at 80 °C, NiFe-LDH also presents higher performance than that of IrO_x, reaching a 74.7% conversion efficiency and a cell voltage of 1.59 V under working conditions of 1.0 A cm^{-2} (Figure 7f).

NiFe-LDH has been widely studied since the publication of Koshikawa et al. in 2020[89,90] and its poor electrical conductivity has been a challenge. This issue is often dealt with by hybridizing NiFe-LDH with carbonaceous materials, which unfortunately decreases the overall stability of the catalyst. Sun et al. found a solution to improve the conductivity without using carbonaceous materials in 2021. They deposited a monolayer NiFe-LDH on Ni foam which gives the catalyst a better conductivity than that of the conventional bulk NiFe-LDH, allowing a 72.6% conversion efficiency with a stability over 50 h at a current density of 1 A cm^{-2} in 1 M KOH AEMWE at 50 °C.[90a] Following this idea, in 2022, Klingenhof et al. tuned NiFe-LDH on Ni foam with anions such as CO_3^{2-}, Cl^-, and ClO_4^- (**Figure 8a–i**), which increases the half and single cells activities (Figure 8j,k). The improvements go up to 91-fold and 2-fold compared to the original NiFe-LDH-coated Ni foam for the 3LC cell and the AEMWE single cell, respectively (Figure 8l). It reached a current density of 587 mA cm^{-2} at a cell voltage of 1.52 V in a 5 cm^2 AEMWE single cell.[89]

The insufficient mass transfer of the anode catalyst for OER limits the overall water electrolysis performance (i.e., catalytic activities and lifetimes) at industrial-level related current densities. A recent study by Li et al. revealed that porous hierarchical structure engineering of the Ni-Fe electrocatalyst could promote the mass transfer for OER in water electrolysis, thus resulting in exceptional long-term durability.[32a] The authors employed a seed-assisted heterogeneous nucleation approach to fabricate a dense porous interlayer between the Ni foam substrate and the flowerlike porous catalyst layer (CAPist-L1). This CAPist-L1

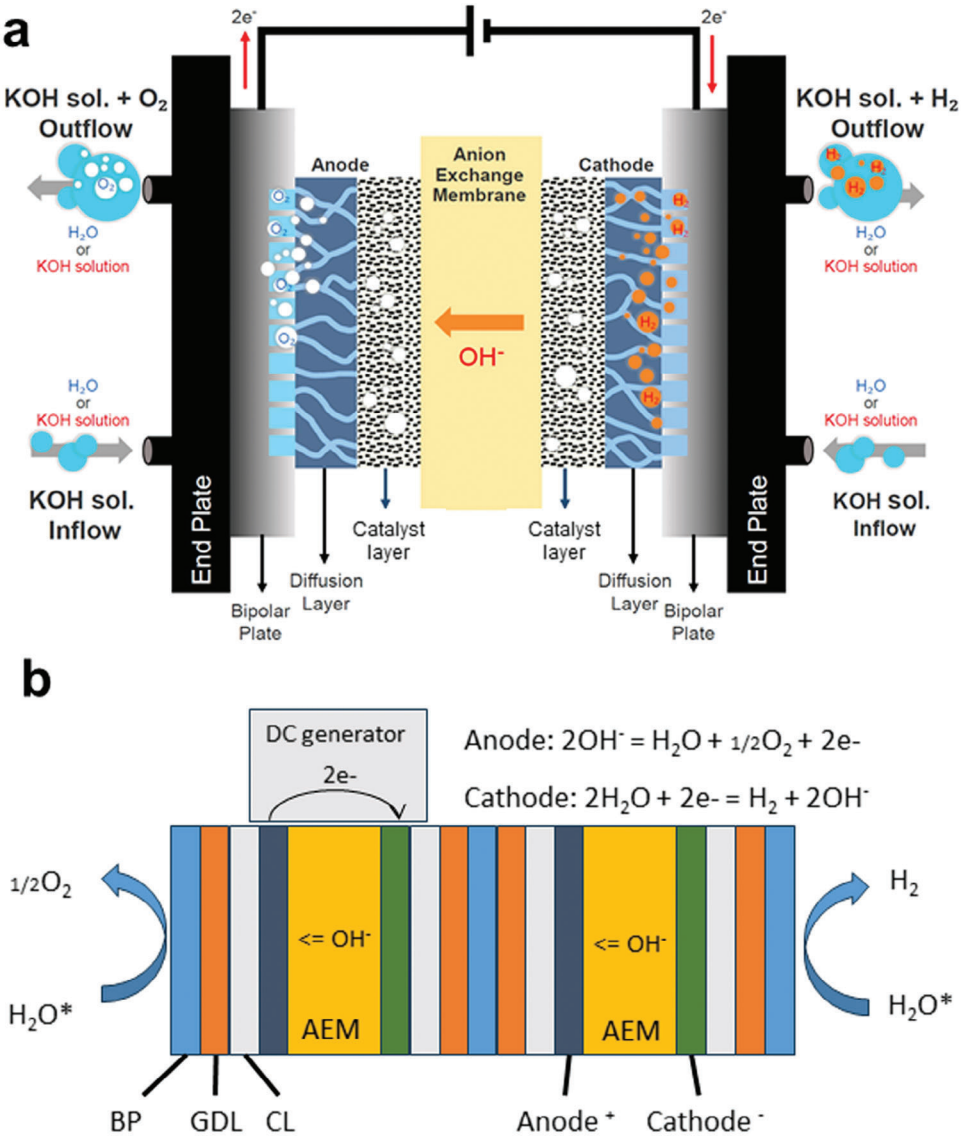

Figure 6. a) The diagram of an AEMWE cell. Reproduced with permission.[82] Copyright 2020, Elsevier B.V. b) AEMWE two cells representation extracted from a stack (*: The water flow can come from both electrodes or only from one[18b,83]).

ensures long-term durability of 15 200 h (over 21 months) in a 3LC cell at 1000 mA cm^{-2} in 1 M KOH. When applied as the anode catalyst in AEMWE, it offered a current density of 7350 mA cm^{-2} at a cell voltage of 2.0 V. Besides, a 1500 h stability was also achieved at 1000 mA cm^{-2} at 80 °C in the CAPist-L1 AEMWE.

2.3.2. Cathode Engineering

Ni and Mo-Based Cathode Catalysts: As previously mentioned, HER does not occur as easily as OER in an alkaline environment. The most active and stable HER catalysts for AEMWE to date are the nanometric Pt-Ni[91] and Pt/C catalysts.[92] Fortunately, same as OER, HER in AEMWE can use non-noble metal at the cathode side as well. For now, the most promising non-noble HER catalyst seems to be a Ni-Mo-based one.[85,92b,93] Although Ni-based electrocatalysts are less active than noble metal-based catalysts when normalized by volume or surface area, it is generally possible to achieve a similar overpotential with higher loads without any impact on cost since Ni is much cheaper than Pt.[92c] Chen et al. applied the Ni-Mo catalyst for both OER and HER (Fe-NiMo-NH_3/H_2 for OER and NiMo-NH_3/H_2 for HER). Integrated into an AEMWE, these catalysts delivered 1.0 A cm^{-2} at a cell voltage of 1.57 V at 80 °C in 1 M KOH with an energy conversion efficiency of 75%.[94] Another study from Bartoli et al. highlights the impact of MoO_2 on the HER catalyst activity.[95] The authors fabricated MnO_2 catalysts from $MoNiO_4$ nanorod arrays. The surface polycrystalline MoO_2 layer played a key role in the HER activity enhancement, demonstrating a current density of 0.55 A cm^{-2} at a cell voltage of 2 V in AEMWE for more than 300 h at 60 °C. Moreover, this catalyst synthetic procedure was also scaled up to

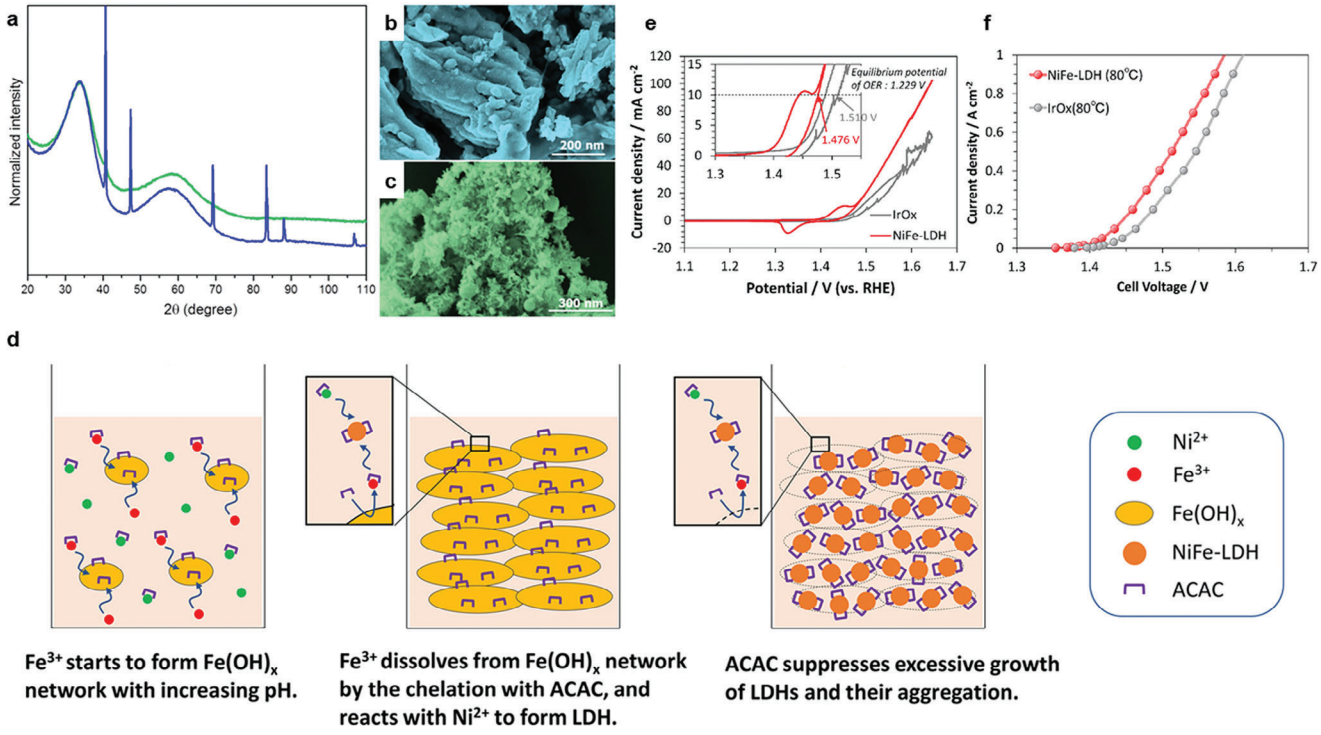

Figure 7. a) The XRD pattern of the synthesized IrO_x (green) and the commercial IrO_x (blue); b and c) The SEM images of the commercial IrO_x and synthesized IrO_x catalysts, respectively. Reproduced with permission.[87] Copyright 2017, American Chemical Society. d) The schematic of the synthetic mechanism of NiFe-layered double hydroxide (LDH). e) Current-voltage curves. The inset: magnified curves. f) Current-voltage plots of MEAs with NiFe-LDH (red) and IrOx (gray) as anode catalysts at 80 °C. Reproduced with permission.[88] Copyright 2020, American Chemical Society.

fabricate electrodes with an area of 78.5 cm^{-2}, which were further employed in an AEMWE stack of three cells.

With this knowledge, it seems logical to combine NiMo and MoO_2. Zhang et al. fabricated the $MoNi_4/MoO_2$@NF (**Figure 9a**) catalyst and employed it in a water-alkali electrolyzer.[96] $MoNi_4/MoO_2$@NF (noted as $MoNi_4$ in Figure 9b–e) demonstrates a 0 mV onset potential that is comparable to that of Pt catalyst (Figure 9b,d). The Tafel slope analysis shows that $MoNi_4/MoO_2$@NF follows the same kinetic rate-limiting step as that of the Pt catalyst (Figure 9c). Besides, $MoNi_4/MoO_2$@NF surpasses Pt catalyst at high current density conditions (Figure 9b,c), with robust durability after a period of 10 h (Figure 9e). Density function theory (DFT) illustrates the kinetic energy barriers of the prior Volmer step (ΔG_{H2O}) and the concomitant combination of adsorbed H into molecular hydrogen (ΔG_H, Tafel step) on Ni, Mo, MoO_2, and $MoNi_4$ (**Figure 10a**). $MoNi_4$ has the lowest ΔG_{H2O} among all the samples and a low $|\Delta G_H|$, providing a fast Tafel step (Figure 10b,c). This $NiMo/MoO_2$ catalyst seems to be the state-of-the-art catalyst for alkaline cathode[97] and has been used in the AEMWE stack. With Ni_2Fe_8–Ni_3S_2/NF as an anode and Ni_4Mo/MoO_2/NF as a cathode, it offers high AEMWE performance (1.65 V @ 1 A cm^{-2}) and high durability (100 h @ 1 A cm^{-2}).[98]

Mn-Fe-Ni-Based Bifunctional Catalysts: Utilizing bifunctional catalysts (i.e., the same catalyst for both the anode and the cathode) is also another option to simplify the electrolyzer design, offering extra opportunities to reduce the cost. This technology is the subject of particular interest in terms of publications, several of which have been published recently.[85,99] Our previous work of MnO_x-decorated Ni-Fe phosphides nanosheets on Ni foam (MnO_x/NiFeP/NF, **Figure 11a**) as the bifunctional catalyst allows the robust symmetric overall water splitting with a current density up to 1000 mA cm^{-2}.[99c] As depicted in Figure 11b–f, the three-step synthetic process successfully fabricates the MnO_x/NiFeP on NF without forming aggregated MnOx particles, providing a highly porous substrate structure with evenly distributed metal elements. MnO_x/NiFeP/NF exhibits exceptional bifunctional electrochemical performance toward water splitting with an overpotential of 255 mV for HER and an overpotential of 296 mV for OER at 500 mA cm^{-2}. It makes MnO_x/NiFeP/NF ideal for the symmetric cell operation of water splitting, which facilitates large-scale industrial operation. Being employed as both cathode and anode in the symmetric cell, MnO_x/NiFeP/NF allows the overall-water-splitting performance with 1000, 500, and 100 mA cm^{-2} at cell voltages of 1.828, 1.796, and 1.686 V, respectively (Figure 11g). Besides, Figure 11h also demonstrates the robust durability of MnO_x/NiFeP/NF in the symmetric water splitting cell of 120 and 100 h at 500 and 100 mA cm^{-2}, respectively. This MnO_x/NiFeP/NF stands out among many transition-metal-based HER, and OER bifunctional catalysts (Figure 11i).

In industrialization, the direct electrolysis of seawater would further decrease the expense of the operation. Based on the same concept, our group proceeded with the design of the bifunctional Mn-doped Ni_2P/Fe_2P catalyst for the overall seawater splitting.[100] Combined with hydrothermal and phosphorization

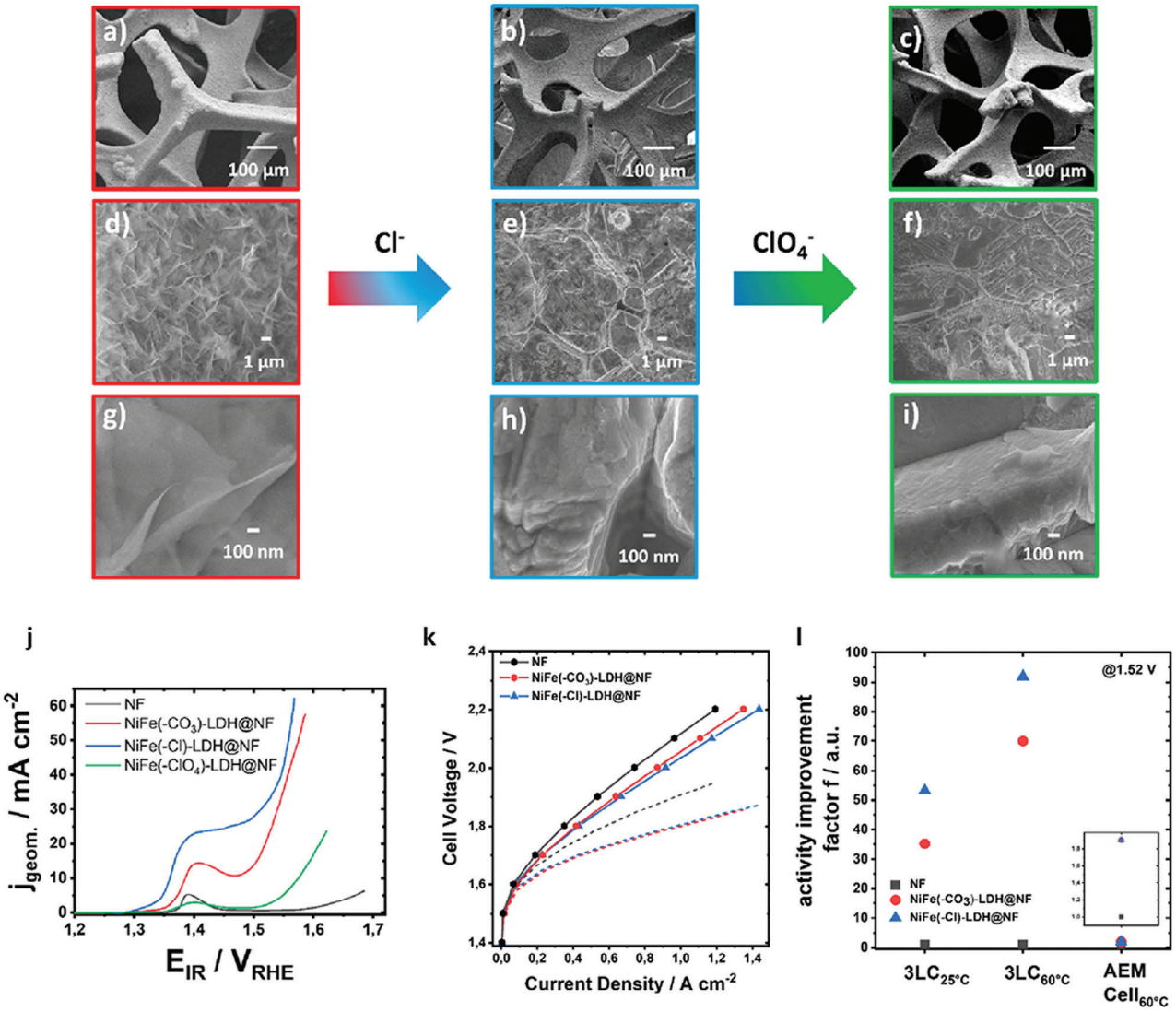

Figure 8. The SEM images of the fabricated anode materials: a,d, and g) NiFe(–CO_3^{2-})-LDH@Ni foam (NF) (red), b,e, and h) NiFe(–Cl^-)-LDH@NF (blue), and c,f, and i) NiFe(–ClO_4^-)-LDH@NF (green). j) iR-corrected linear sweep voltage (LSV) analyses of OER performance at 60 °C of NiFe(-CO_3^{2-})-LDH@NF (red), NF (black), and NiFe(-Cl^-)-LDH@NF (blue)) at room temperature in 0.1 M KOH. k) The polarization curves of NiFe(-CO_3^{2-})-LDH@NF (red) and NiFe(-Cl^-)-LDH@NF (blue), and NF (black) in AEMWE single cell. Dashed lines: iR-corrected curves. l) The comparisons in factors of activity improvement of anion tuning in the three-electrode liquid cell (3LC) at 60 and 25 °C, AEMWE single-cell, and the blow-up (different scale in the y-axis) of the AEMWE single-cell. Reproduced with permission.[89] Copyright 2022, American Chemical Society.

methods, the 3D flower-shaped Mn-doped Ni_2P/Fe_2P on NF can be fabricated with rich element distribution (**Figure 12**a–d). The Mn-doped Ni_2P/Fe_2P catalyst shows high performance with low overpotentials of 357 and 470 mV for OER and HER, respectively, at 1000 mA cm^{-2} in the seawater splitting symmetric cell (Figure 12e–g). Figure 12h,i also demonstrates the excellent HER and OER durability of Mn-doped Ni_2P/Fe_2P, making these Mn-Ni-Fe bifunctional water-splitting catalysts promising for future applications.

To achieve significant electrolysis performance, the other main component studied is the membrane and its related elements.

2.3.3. Electrolyte, Membrane, and Ionomer Engineering

The AEM roles are to transport the OH^- ions, separate the O_2 and H_2 products, and be a barrier between the two electrodes for the electrons. The AEM is composed of a polymer backbone, responsible for mechanical and thermal stability, and a functional group that transports the OH^- anion, responsible for the ionic conductivity, ion exchange capacity, and transport number.[15b] The ideal AEM and ionomer must have high conductivity and durability as well as strong mechanical properties.[83a,84c,85,92b,c,101] The details of AEM characterization methods are described in a previous review.[19a]

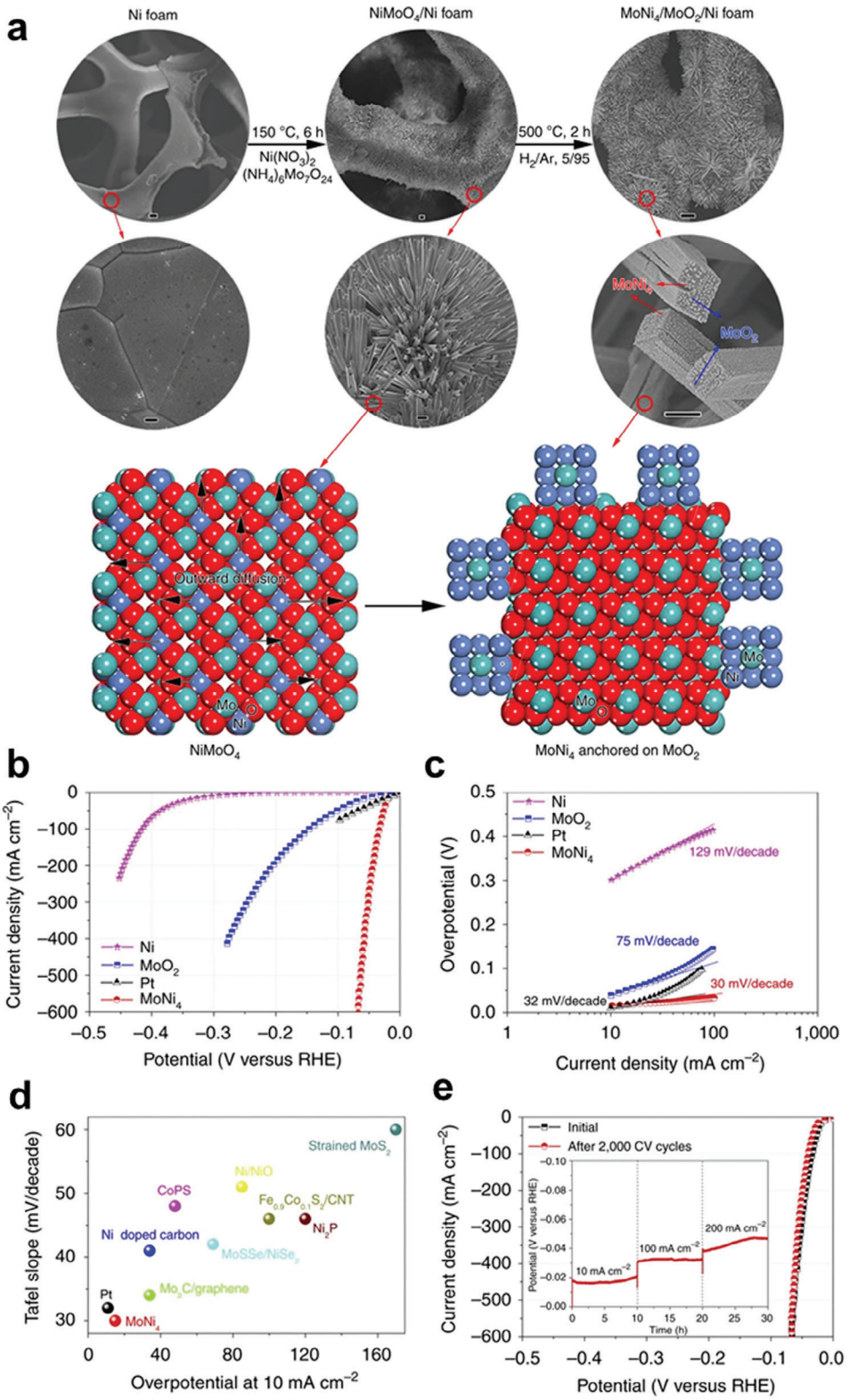

Figure 9. a) The synthetic route of $MoNi_4$ supported by MoO_2 cuboids on NF. Scale bars, NF: top-20 µm and bottom-1 µm; $NiMoO_4$/NF: top-10 µm and bottom-2 µm; $MoNi_4/MoO_2$/NF: top-20 µm and bottom-1 µm. b) The polarization and c) Tafel plots of the pure Ni nanosheets, $MoNi_4$ supported by MoO_2 cuboids, and MoO_2 cuboids on NF. d) The comparative chart of the state-of-the-art HER electrocatalyst materials. e) The polarization plots of $MoNi_4$ before and after 2000 cycles of cyclic voltammetry; inset: durability tests of $MoNi_4$ at 10, 100, and 200 mA cm^{-2} with a scan rate of 1 mV s^{-1} in 1 M KOH. Reproduced under terms of CC BY 4.0 license.[96] Copyright 2017, Jian Zhang et al., published by Springer Nature.

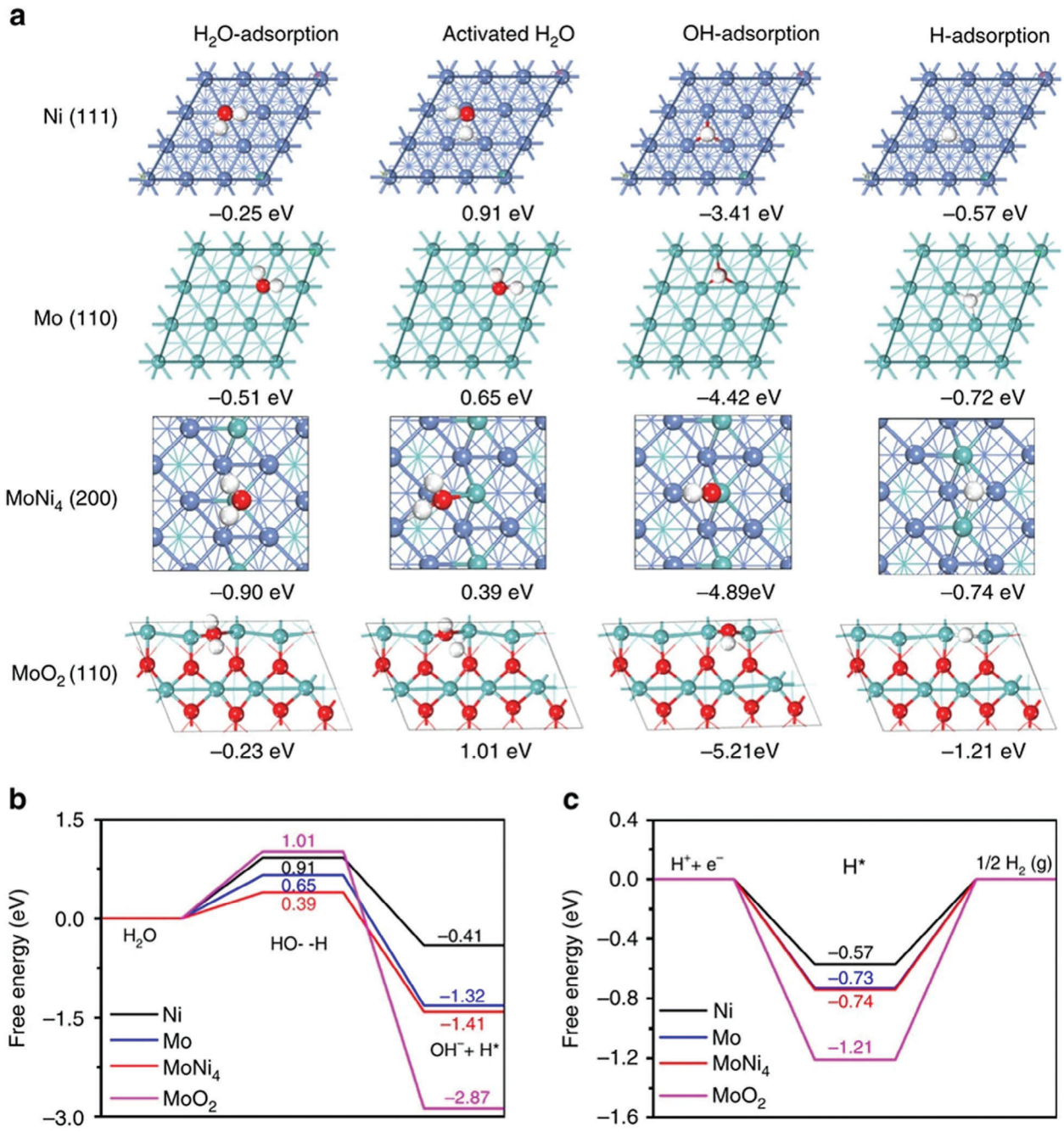

Figure 10. a) The free energy calculations of H adsorption, H_2O adsorption, activated H_2O adsorption, and OH adsorption. The adsorption-free energy calculation diagram for b) the Volmer step and c) the Tafel step. Aqua balls: Mo; Blue balls: Ni; Red balls: O. Reproduced under terms of CC BY 4.0 license.[96] Copyright 2017, Jian Zhang et al., published by Springer Nature.

Polymer Membranes: A recent study published in 2021, affirms to have achieved the best current density and durability for AEMWEs (**Figure 13a**) using four types of poly(fluorenyl-co-aryl piperidinium) (PFAP, Figure 13b–e) copolymers in an anhydrous cathode system.[102] They obtained a current density of 7.68 A cm^{-2} at 2.0 V and 80 °C (Figure 13g), using PGM catalysts with 1 M KOH feed at the anode, which is better than the state-of-the-art PEMWE (6 A cm^{-2} at 2.0 V[103]). Without PGM, the AEMWE still exhibits the outstanding performance of 1.62 A cm^{-2} at 2.0 V and 80 °C (Figure 13f). Compared to most of the other AEMs that give AEMWEs poor current density (below 4 A cm^{-2} at 2.0 V) and/or cell durability (<100 h), this PFAP copolymer membrane enables PGM and PGM-free AEMWEs to be stable for more than 1000 h, according to in-situ characterization, under a 0.5 A cm^{-2} current density at 60 °C (**Figure 14a–d**).

With an anhydrous cathode, this special system requires excellent water diffusion from the ionomer and AEM to supply H_2O

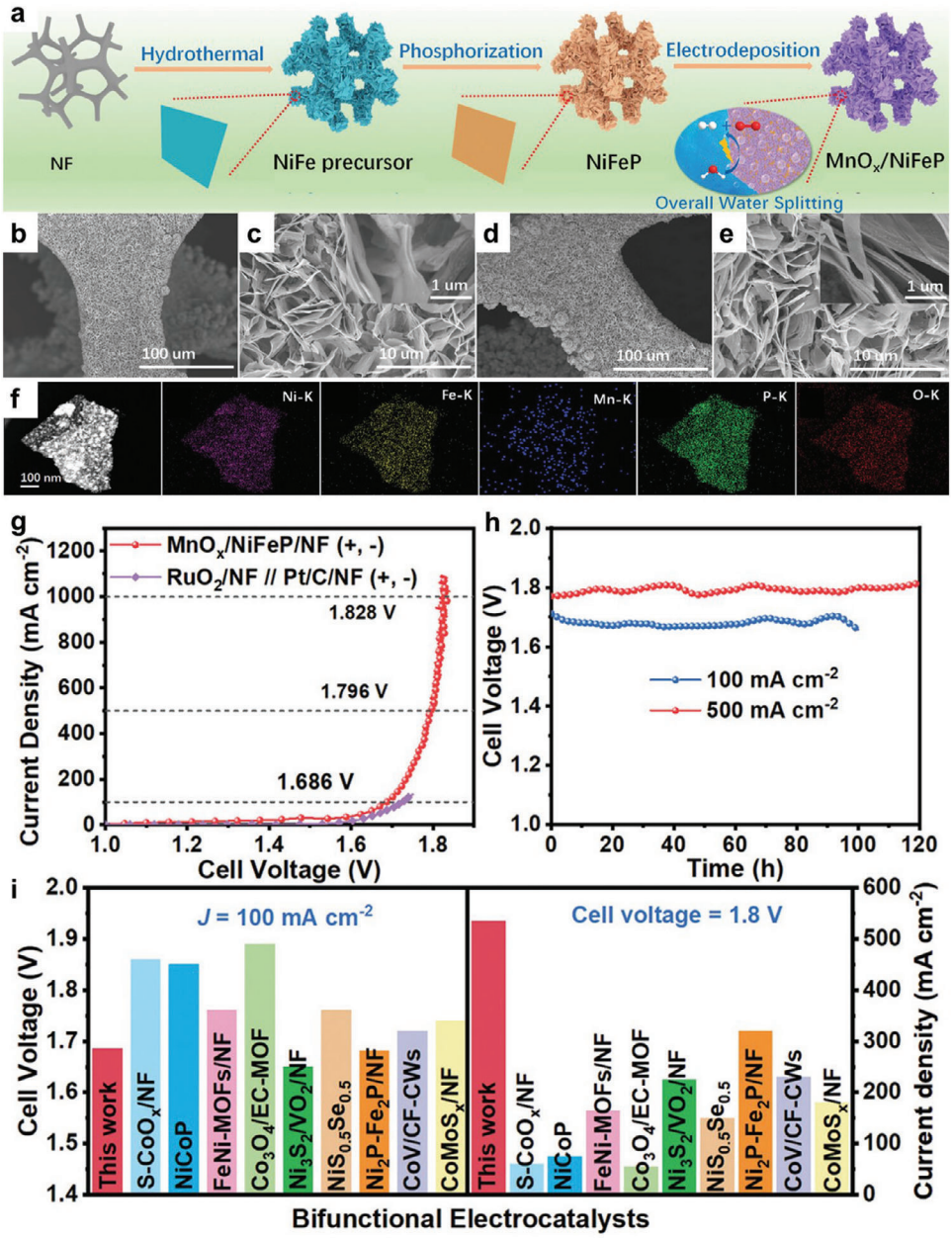

Figure 11. a) The synthetic route of MnO_x/NiFeP/NF. The SEM images of b and c) NiFeP/NF and d and e) MnO_x/NiFeP/NF. f) The STEM image and corresponding elemental mapping images of MnO_x/NiFeP. g) The overall water splitting polarization plots of RuO_2/NF//Pt/C/NF and MnO_x/NiFeP/NF. h) The durability test of MnO_x/NiFeP/NF at 500 and 100 mA cm^{-2} in a two-electrode cell configuration. i) The comparison of 100 mA cm^{-2} current densities and 1.8 V cell voltages of different bifunctional electrocatalysts for overall water splitting, respectively. Reproduced with permission.[99c] Copyright 2021, Wiley-VCH GmbH.

to the cathode. For this reason, PFBP-14 was chosen as the cathode ionomer for its high performance in water diffusivity and ion exchange capacity (IEC). The optimized ionomer content within the AEMWE was found to be 25%, giving a current density of 7.68 A cm^{-2} (Figure 13g). PFTP-8 as the anode ionomer provides great IEC and low water diffusivity. PFTP-13 as the AEM achieves a high current density (Figure 13e,f) and high stability (Figure 14a,b). 1 M KOH was chosen as the electrolyte since a high electrolyte concentration considerably reduces the overpotential at a high current density.[84a] More details are studied on the impact of electrolyte feed in the following research.[104]

AEM and ionomer are considered among the most difficult to research for AEMWE, as they degrade at high temperatures under basic conditions and are therefore responsible for the poor stability and durability of AEMWEs.[83a] Some companies (e.g., Dioxide Materials) have been working on the commercialized AEM and obtained some pioneering results. For example, their sustainion@37-50 AEM allows an AEMWE operation

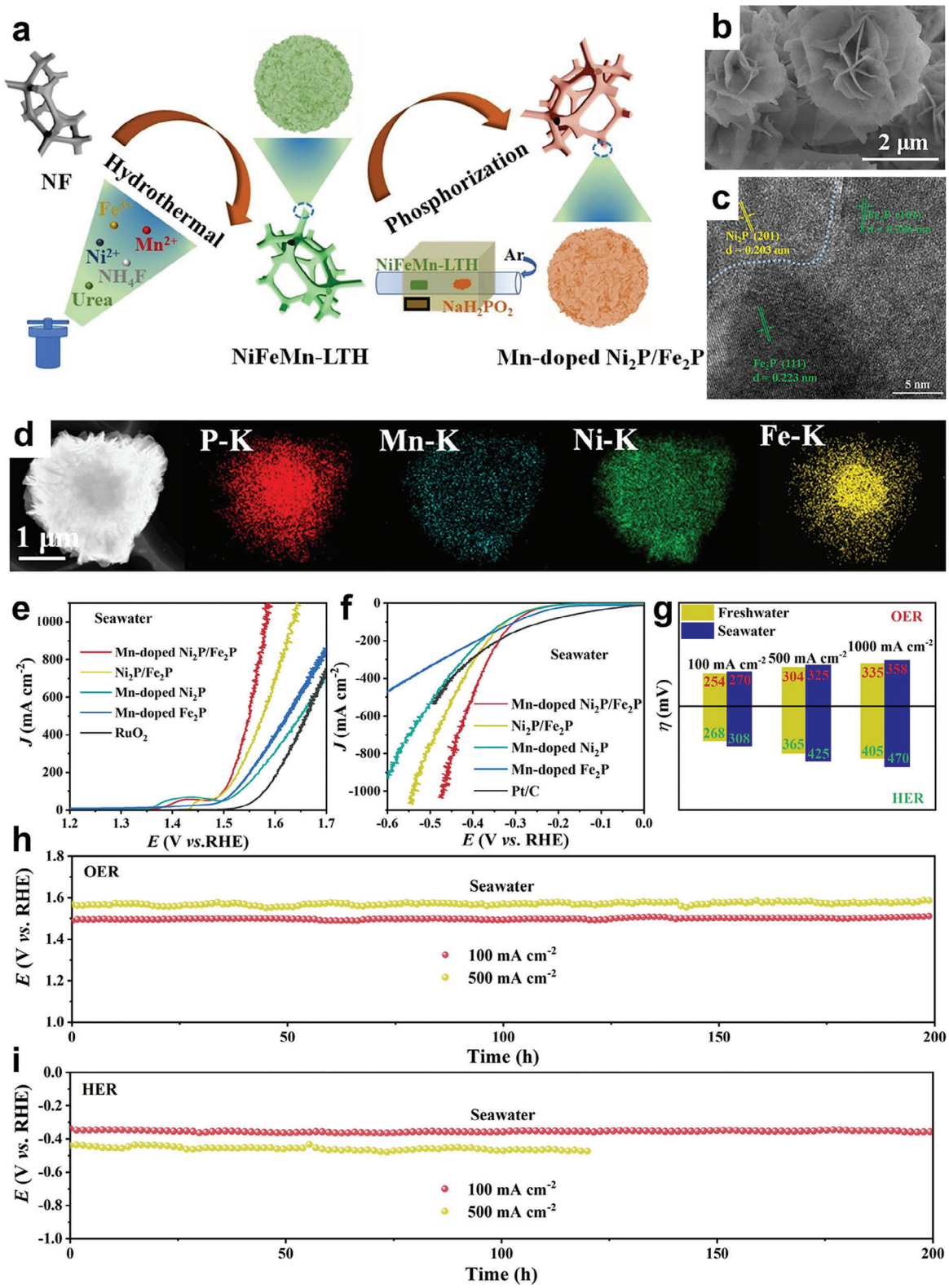

Figure 12. a) The schematic of the synthesis of Mn-doped Ni_2P/Fe_2P. b) The SEM image of Mn-doped Ni_2P/Fe_2P. c) The TEM image of Mn-doped Ni_2P/Fe_2P. d) The HAADF-STEM image and its corresponding element mapping EDS images of Mn-doped Ni_2P/Fe_2P. Scale bar: 1 μm. e) The OER polarization plots of the prepared catalysts tested in alkaline seawater. f) The HER polarization plots of the prepared catalysts tested in alkaline seawater. g) The overpotential comparison of Mn-doped Ni_2P/Fe_2P at 500 and 100 mA cm^{-2} measured in seawater and alkaline freshwater. h) OER and i) HER durability measurements of Mn-doped Ni_2P/Fe_2P under the alkaline seawater condition. Reproduced with permission.[100] Copyright 2022, Elsevier B.V.

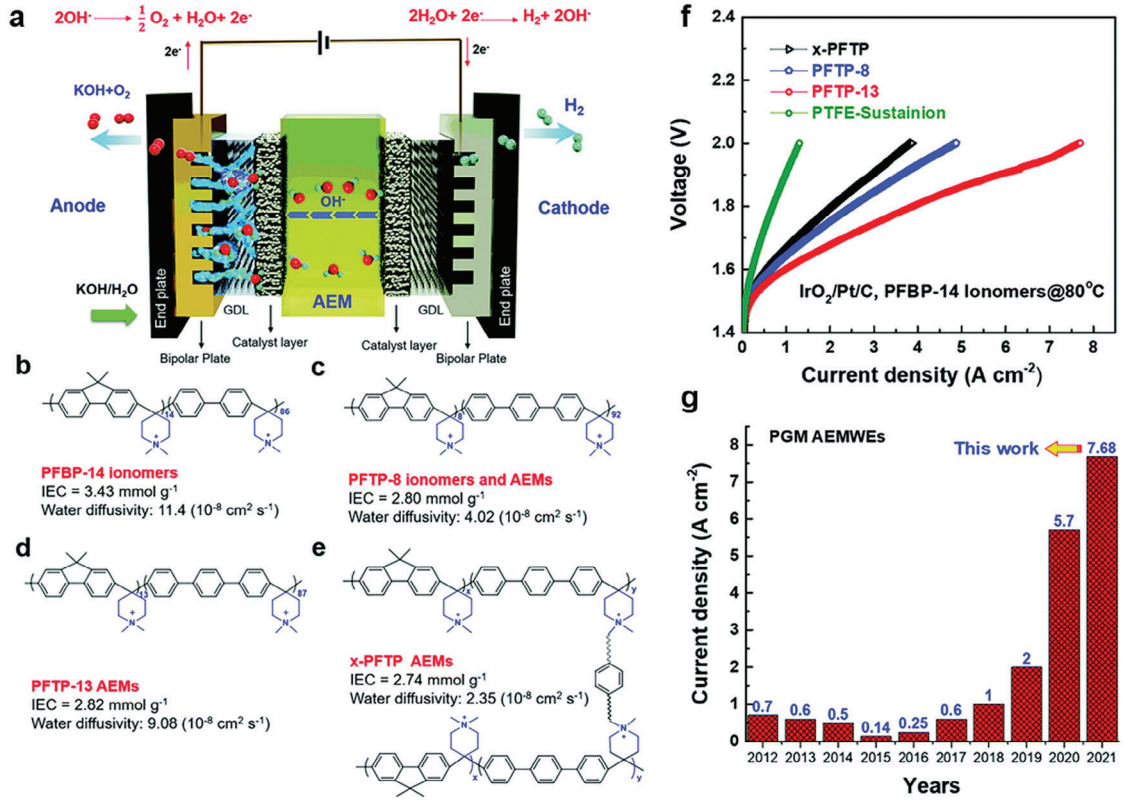

Figure 13. a) The schematic of the AEMWE, where CL consists of the catalysts and ionomers, b) PFBP-14, c) PFTP-8, d) PFTP-13, and e) cross-linked PFTP. f) The current voltage plots at 80 °C. g) Current density value data of AEMWEs from 2012 to 2021. Reproduced with permission.[102] Copyright 2021, Royal Society of Chemistry.

up to 2000 h at 60 °C in 1 M KOH.[105] Notice that the anion conductive sustainion@ series membrane can also be employed for other electrolyzers such as CO_2 electrolyzer[106] and photovoltaic-electrolyzer.[107] Although at a low current density (50 mA cm^{-2}), the sustainion@ membrane allowed a 6-month operation of CO_2-CO in an alkaline CO2 electrolyzer with CO Faradaic efficiency maintaining ≈90%.[106] The progress of AEM development holds a big opportunity to contribute to the net-zero emission blueprint.

In short, the three main components of the AEMWE, the two electrocatalysts, and the AEM, have already been discussed. They need to be successfully linked to form an efficient stack to offer industrial-level-related activities.

2.3.4. Optimizing the System Configurations

Most of the subjects concerning AEMWEs are inherited from, or similar to, PEMWEs. For the AEMWE MEA manufacturing process, CCM and CCS are directly derived from PEMWE. The CCM approach for PEMWE is also preferred for AEMWEs, as it enables higher ionic conductivity to be maintained.[18b] However, due to rigorous operating conditions, CCM is mainly used in laboratories whereas CCS is preferred in industrial processes.[70] It is therefore necessary to develop one specifically for AEMWEs. Park et al. studied the effects of the MEA fabrication process as well as operating conditions on cell performance using commercial materials such as FAA-3-50 and FAA-3-Br as the AEM and anion exchange ionomer, respectively.[108] The cathode side was made of Pt/C CL and carbon GDL while the anode side was made of IrO_2 CL and Ti GDL (**Figure 15**a,d). As highlighted in previously discussed studies, this one also found the CCM process to be more effective than the CCS process (Figure 15b,c). Concerning the electrolyte feed, the best performance was obtained with 1 M KOH at both the anode and the cathode and with a flow rate of 2.5 ml min^{-1} (Figure 15e,f).

The optimal ionomer content was 20 wt.% (**Figure 16**a–c) and the cell temperature was optimal at 70 °C (Figure 16d,e) over which the AEM started degrading. Concerning the GDL thickness it was optimal at 350 and 420 µm for the Ti-GDL and the C-GDL respectively (Figure 16f,g). Those optimized AEMWE parameters allowed the catalytic enhancement up to 6-fold compared to other reports.[108]

However, this fabrication process and operating conditions are optimal for this AEMWE. The optimal conditions for different materials and MEA systems might change.

A recent study on Ni-based GDL[109] concluded that NF offered the best performance in terms of compromise between electrical conductivity and mass transfer, as well as better durability and stability than those of Ti-based GDL.

Many cases of water electrolysis are conducted at a very restricted set of conditions. There is no standard to test AEM performance. **Table 2** lists some examples of AEMWE studies with various experimental conditions. The components, setup, and

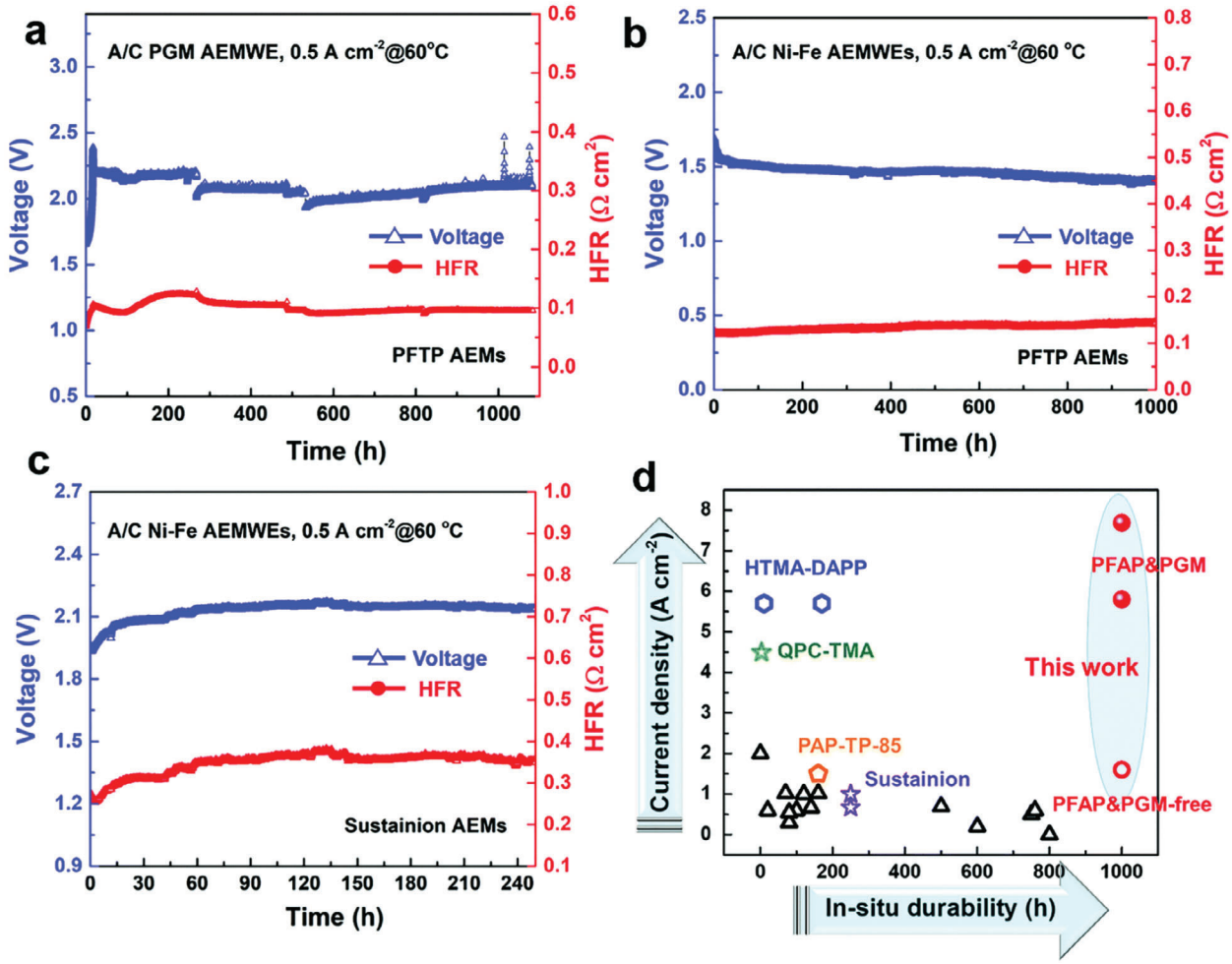

Figure 14. In situ durability of a) PFTP-13-PGM AEMWE with IrO_2 anode (2 mg cm^{-2}) and Pt/C cathode (0.5 mg cm^{-2}), b) PFTP-13-A/C Ni–Fe AEMWE and c) PTFE-reinforced Sustainion®-A/C Ni–Fe AEMWE at 60 °C under 0.5 A cm^{-2}; d) The current densities and in-situ durability of state-of-the-art AEMWEs. Purple stars denote the commercial Sustainion® AEMWEs used in the presented work; red circles denote the PFAP-based AEMWEs in the presented work; the green star denotes a poly(carbazole)-based AEMWE; blue hexagons denote typical hexamethyl trimethyl ammonium-functionalized Diels–Alder polyphenylene (HTMA-DAPP)-based AEMWEs; the orange pentagon denotes a PAP-TP-85-based AEMWE; and black triangles denote other AEMWEs. Reproduced with permission.[102] Copyright 2021, Royal Society of Chemistry.

assembly of AEMWE (e.g., catalyst nature, mass loading of the catalyst, membrane, electrolyte, etc.) are all essential to the final catalytic performance (i.e., current density, overpotential/cell voltage, stability, etc.). In different reports, the experimental conditions such as operating temperature, catalyst loadings, applied membrane, and target current density for stability tests differ. It leads to difficulty when trying to compare different studies that did not use the same protocol. Thus, it is urgent to implement a standard test to enable clear and full comparison for novel electrocatalysts in AEMWE as proposed by Faqeeh et al. in ref. [110].

Materials for specific use in AEMWE are at an early stage of development, as most previous studies have been carried out on AEM fuel cells.[102] However, the characteristics and related issues are almost identical.[54] With the recent breakthroughs, some industries (e.g., Enapter) have already commercialized their AEMWE systems from 2.4 kW up to 100 MW worldwide, which is applied in various industries such as power supply and agriculture.[112] It demonstrates the promise and importance of AEMWE in the future hydrogen ecosystem.

3. Electrolyzers, Reverse Mode: Fuel Cells, and Reversible Mode: Regenerative Fuel Cells

Research on fuel cells (FCs) and regenerative fuel cells (RFCs) is crucial for developing the next stage in the hydrogen ecosystem after its production. Meanwhile, challenges for FCs and RFCs are similar to those of the HER electrolyzers, leading to scientific discoveries that could be useful for both HER electrolyzers and FC (e.g., in situ characterization techniques).[54,113]

3.1. Electrolyzers in Reverse Devices: Fuel cells

Fuel cell (FC) works in the opposite way of the water electrolyzer (Equation 4). They change chemical energy into electrical and

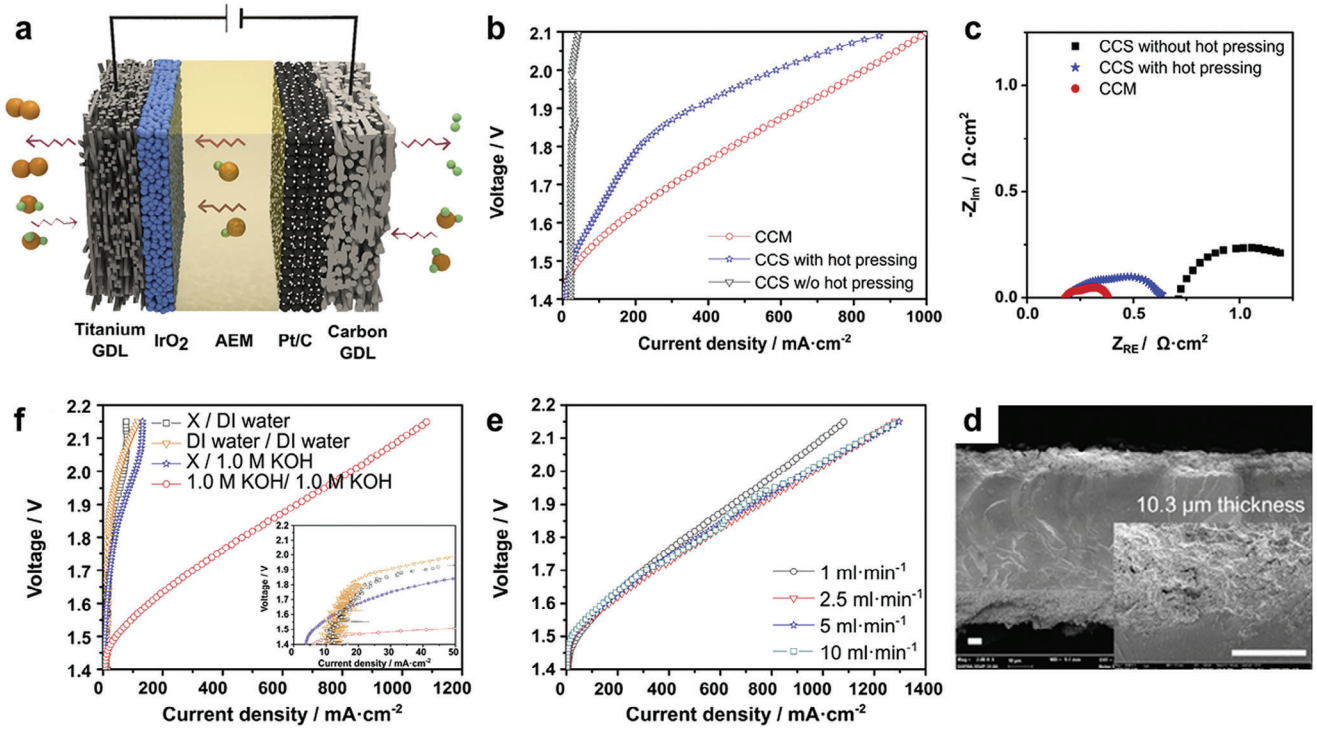

Figure 15. a) The schematic of an AEMWE single-cell. b) The polarization plots and c) Nyquist curves for AEMWE single cells under different fabrication methods: CCM and CCS without and with hot-pressing at 50 °C. d) The SEM images of MEAs cross-sections with a 4 mg cm^{-2} anode catalyst loading. Scale bar: 5 μm. e) The AEMWEs cell performance with different 1 M KOH flow rates on both sides of the electrode (1, 2.5, 5, and 10 ml min^{-1}). f) The polarization plots for AEMWEs operated under different reactant flow rates. Reproduced with permission.[108] Copyright 2018, Elsevier Ltd.

thermal energy. For example, the PEM FC system operates as follows: at the anode, the H_2 molecule on a catalyst decomposes itself in protons and free electrons that create the electric current (Equation 5). At the cathode, O_2 reacts with the freed electrons (Equation 6). Finally, protons recombine with oxygen ions when they arrive at the cathode to make water (Equation 7). PEM FC is the most currently used FC.[114] Other FCs are applied to different situations such as acid electrolytes (i.e., PEM FC, Direct Methanol Fuel Cell (DMFC), Phosphoric Acid Fuel Cell (PAFC)) and basic electrolytes (i.e., SOFC, Alkaline Fuel Cell (AFC), Molten Carbonate Fuel Cell (MCFC)),[115] as listed in **Table 3**.

$$2H_2 + O_2 => 2H_2O + \text{electricity} + \text{heat} \quad (4)$$

$$H_2 => 2H^+ + 2e^- \quad (5)$$

$$O_2 + 4e^- => 2O^{2-} \quad (6)$$

$$4H^+ + 2O^{2-} => 2H_2O \quad (7)$$

PEMFCs and SOFCs are considered the most promising. However, the PEMFC operates at a too-low temperature, while the SOFC operates at a too-high temperature. To counter these disadvantages, a protonic ceramic fuel cell (PCFC) is studied as it works at intermediate temperatures. Another rather recent FC is the AEM FC with a high improvement potential.[117] The challenges for FC are quite like those for electrolyzers (i.e., improving material designs).

One of many applications of the FC is their stationary use in the electrical grid thanks to the power-to-gas conversion previously made by the HER electrolyzer. When electricity production exceeds demand, electrical energy can be converted into H_2 for long-term storage by electrolysis. When electricity production is low, it would be desirable to convert the chemical energy in H_2 back to electricity by FC. This process requires power plants capable of both electrolysis and FC operation, a technology known as regenerative fuel cell (RFC).

3.2. Electrolyzers in Reversible Devices: RFC

The RFCs are used for energy storage and conversion but for now only in military and aerospace areas because of their high price.[119] There are two types of RFCs: discrete and unitized RFCs (DRFC and URFC, respectively). In a DRFC, the electrolyzer and FC work relatively independently, as represented in **Figure 17a**.

In URFC, the electrolyzer and FC are combined in one cell, which forces the electrodes to be bifunctional. For URFC, there are two types of operating configuration: the constant gas (CG) and the constant electrode (CE) (Figure 17b,c). URFC in CE mode demonstrates better performance than those of DRFC or URFC in CG mode.[118] PEM FC, AFC, and SOFC are three main FCs that are reversible, forming the principal RFC system.[116d] Currently. only UR-PEM FC has achieved a mature level.[119] For electrolyzers, FC, and RFC, the PEM is the key to the challenges of

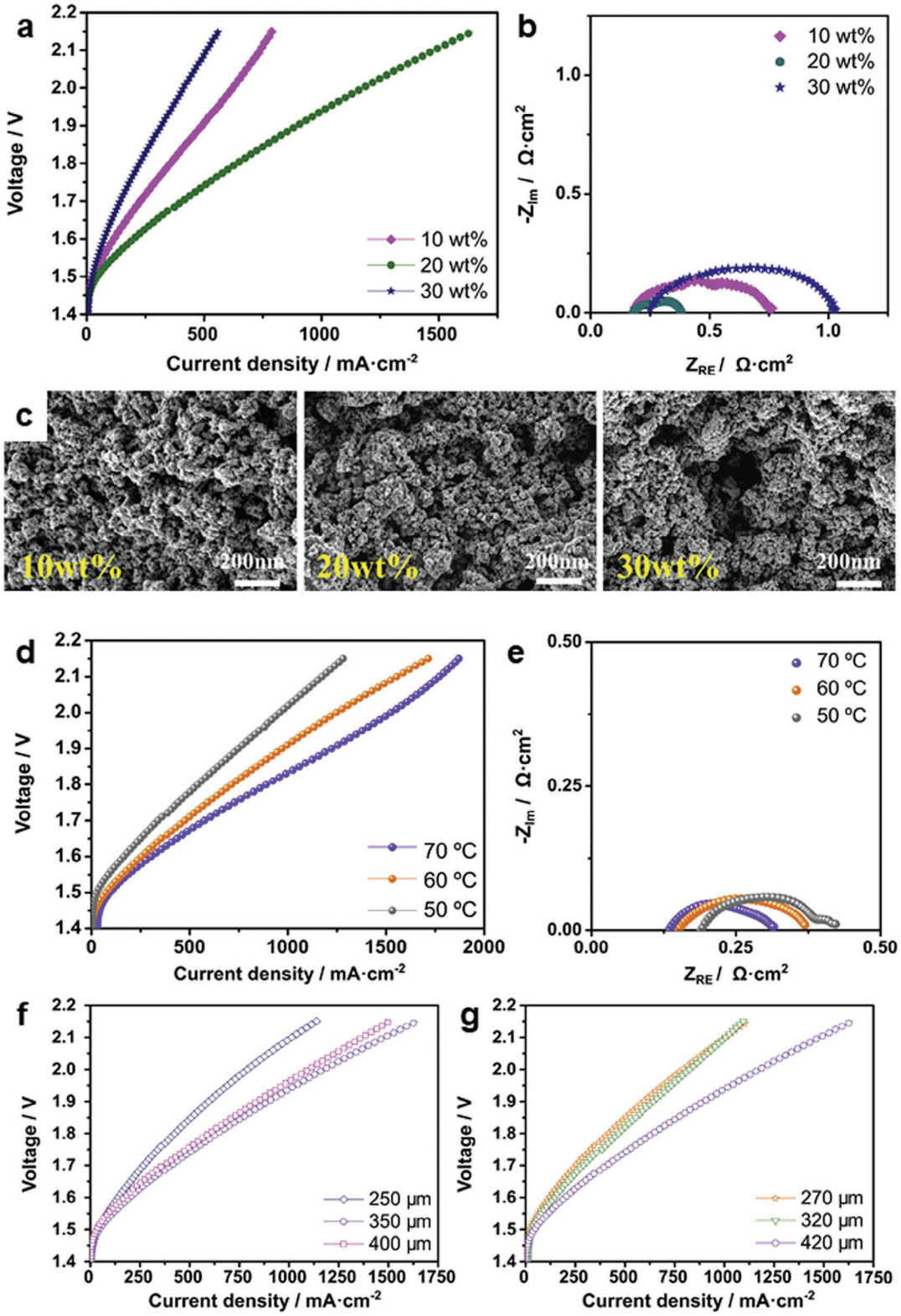

Figure 16. a) The polarization and b) Nyquist curves for AEMWEs with 10 wt.%, 20 wt.%, and 30 wt.% ionomer contents at 50 °C and c) The SEM images of the fabricated MEAs. d) The polarization and e) Nyquist curves for AEMWEs operated at 50, 60, and 70 °C. The polarization plots for single cells with different thicknesses of f) Ti-GDLs and g) C-GDLs at 50 °C. Reproduced with permission.[108] Copyright 2018, Elsevier Ltd.

Table 2. The comparison of AEMWE performances in various conditions.

Catalysts: Anode/Cathode	Catalyst loadings [mg cm^{-2}]: Anode/Cathode	AEM	Current density [A cm^{-2}]	Stability [cell voltage increase < 10%]	Refs.
Stainless steel/Pt/C	Not applicable/0.5	Sustainion@ X37-50	2.74 at 2.0 V at 60 °C	> 25 h at 60 °C at 1 A cm^{-2}	[110]
		FAA-3-50	1.40 at 2.0 V at 60 °C	< 10 h at 60 °C at 1 A cm^{-2}	[110]
IrO_2/Pt/C	2/2	FAA-3-50	1.00 at 1.8 V at 60 °C	< 8 h at 60 °C at 0.5 A cm^{-2}	[111]
	4/0.4	FAA-3-50	1.50 at 1.9 V at 70 °C	Not applicable	[108]
	2/0.5	PFTP-13	7.68 at 2.0 V at 80 °C	> 1000 h at 60 °C at 0.5 A cm^{-2}	[102]

cost reduction to compensate for noble metal materials. **Table 4** lists the advantages and disadvantages of DRFC and URFC. Certain advances can benefit all devices. But to achieve high performance, materials need to be developed specifically for each of them, considering their different features.

3.3. The Hydrogen Ecosystem

With stable and large-scale H_2 production being achievable, the H_2 ecosystem that empowers the global industry to transition to a carbon-neutral blueprint can be put into the picture. This scheme (**Figure 18**[120]) of the US Department of Energy (DOE) represents quite well the H_2 ecosystem at a global scale.[121] In some hydroelectricity-rich regions, such as Québec and Norway (almost 100% of the electric power is hydroelectric), renewable energy is integrated into the electric grid. The excessive electricity can be further converted and stored into clean H_2 by electrolyzer for future applications to reduce greenhouse gas (GHG) emissions.[122] Given its abundant reserves of natural gas, North America tends to be a leading region in the production of blue hydrogen.[123] As pointed out in the introduction, the recent discovery of natural hydrogen reserves, such as the large potential reserve in France, could add a new source to this scheme if other reserves are discovered around the world. For the H_2 applications, studies put much effort into H_2 vehicles, such as H_2-FC cars for daily commuting and H_2-FC heavy-duty trucks for good transport. It shows that the research interest in H_2-FC trucks (HFCTs) has grown rapidly in the past ten years, especially in North America and Europe. The environmental impact, H_2 supply chain, and storage tank system are the hottest concerns of HFCTs.[122a] Take an example, the company "First Hydrogen" has selected the City of Shawinigan (Quebec, Canada) to develop its first green H_2 ecosystem, where the local production of green H_2 and the assembly of zero-emission commercial vehicles are secured and developed.[124] In addition, new sources for importing or exporting H_2 could also be added to this H_2 ecosystem scheme in the future.

4. Conclusion and Perspectives

Low-temperature solid-membrane electrolyzers hold great promise to produce green H_2. Their high reactivity enables them to be coupled with renewable energies. And their ability to produce H_2 directly under pressure makes it easy for storage and transport. This review summarizes recent advances in electrocatalysts for the anode and cathode as well as for the membrane and their assembly in MEAs and stack systems for PEMWE and AEMWE. With the application of noble metal-based (e.g., Pt-, Ir-, Ru-based) catalysts, PEMWE is currently the most advanced of water electrolyzers. However, the high cost the noble metal-catalysts burdens the overall capital expenditure of the cell device. The AEMWE seems to represent the next generation, combining the benefits of PEMWEs and AWEs. Non-PGM catalysts like NiFe-based catalysts reveal exceptional catalytic performance in AEMWE. The difficulty of AEMWE mainly falls on the durability issue that concerns the AEM stability and degradation. Membrane engineering remains the top priority in achieving the long-term operation of both PEMWE and AEMWE. The interdisciplinary benefit between electrolyzer research and its reverse mode, FC, is also highlighted. Despite these considerable achievements, several challenges remain:

Table 3. Comparison of FC, based on.[115,116]

Type	Electrolyte	Anode		Cathode		Ionic species	T [°C]	Application/range
		Input	Output	Input	Output			
PEMFC	Polymer (s)	H_2		O_2	H_2O	H^+	80	Portable, transport/10 mW–1 MW
DMFC	Polymer (s)	CH_3OH	CO_2	O_2	H_2O	H^+	80	Portable, transport/10 mW–1 MW
AFC	Potash (l)	H_2	H_2O	O_2		OH^-	100	Space, Military/1–100 kW
PACF	Phosphoric acid (l)	H_2		O_2	H_2O	H^+	200	Stationary/100–440 kW
MCFC	Molten salt (l)	H_2	$H_2O + CO_2$	$O_2 + CO_2$		CO_3^{2-}	650	Stationary/50 kW–10 MW
PCFC	Ceramic (s)	H_2		O_2	H_2O	H^+	400–600	Transport, stationary/100 W–10 kW
SOFC	Ceramic (s)	H_2	H_2O	O_2		O_2	1000	Stationary/100 W–10 MW

DMFC: Direct Methanol; AFC: Alkaline; PAFC: Phosphoric Acid; MCFC: Molten Carbonate; PCFC: Protonic Ceramic; SOFC: Solid Oxide/(s): solid; (l): liquid.

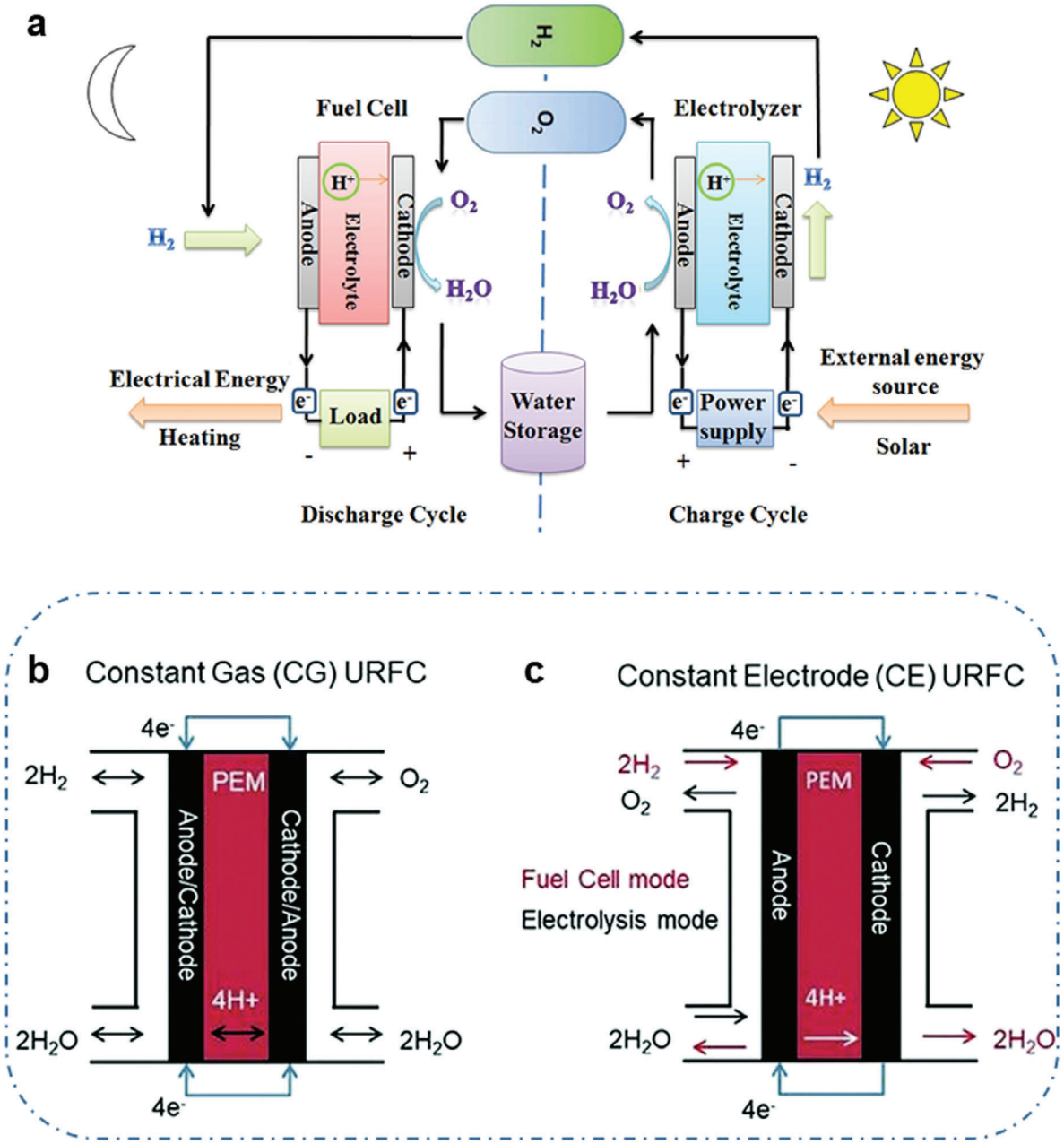

Figure 17. a) The DRFC system, combined with solar energy. Reproduced with permission.[116d] Copyright 2020 Elsevier Ltd. The schematic diagram of b) constant gas and c) constant electrode URFC operating configurations. Reproduced with permission.[118] Copyright 2020, Royal Society of Chemistry.

PEM Challenges

1) Research into PEMWE must focus on BP and GDL, given their large cost contribution and high reduction potential, then comes the manufacturing of the MEA.[15b] 2) Although research is currently concentrating on finding non-noble catalysts for HER and OER, performance is not yet comparable, which leads to the challenge of reducing noble metal loading using technologies such as single-atom catalysts.

AEM Challenges

3) AEMWE research should focus on the membrane and ionomer stability by studying the degradation mechanism via in-situ characterization and by trying to find a balance between the hydroxyl ion conductivity and functional group stability.[101] 4) Research on AEMWE operating in pure water is also considered a future challenge. 5) The AEMWE inherits most of its components from the AWE and PEMWE, which still holds much space for

Table 4. Comparison of URFC and DRFC, based on the publication of Pu et al.[116d]

	DRFC	URFC
Advantages	• Easy amplification, repair, and management • A closed water cycle • Optimized electrolyzer and FC capacities and performances • FC and electrolyzer can operate simultaneously • Cost-effective	• More compact and less heavy system • Less expensive
Disadvantages	• Complex system • Possesses lower volume energy density	• Bifunctional electrodes required
Operating principles	• FC and electrolyzer work independently	• FC and electrolyzer operate alternatively in the same cell
Applications	• Renewable energy storage and conversion • Space • Aircraft • Submarine	• Renewable energy storage and conversion • More employable for space

Electrolyzers, FC, and RFC are only a small part of all the technology used in the hydrogen ecosystem.

improvement for its optimization. Hence, it is necessary to continue research into specific materials for the AEMWE.

Global Challenges

6) There is still no consensus on how to test a new catalyst, membrane, or stack, which makes it very difficult to compare the results of two different research groups. It is therefore urgent for the scientific community to agree on standardized measurements and tests, as well as on a rating grid for grading different types of components. This grid should take into consideration the cost, stability, durability, efficiency, and all the other significant characteristics such as the manufacturing complexity. 7) Too little research has been done on complete stack systems, although this is the ultimate industrial goal. The results from laboratory tests such as a three-electrode system should be implanted into a complete stack system for progress.

Perspectives

8) The research should focus on the area with interdisciplinary benefits such as the characterization method (e.g., in situ or operando technique) to better understand the mechanism and the electricity cost. 9) As aforementioned, direct seawater electrolysis has gained much attention these days. Although intriguing, there are rising arguments on whether direct seawater electrolysis provides significant economic, environmental, and technological incentives for the water electrolysis industry.[125] Detailed and comprehensive analyses should be carried out to offer accurate insights for global orientation in the H_2 production industry. 10) With membrane engineering being one of the biggest challenges in water electrolysis, membrane-less electrolyzers might represent an option to reduce the capital cost. A few years ago, Esposito wrote a nice perspective on the topic in which he proposed some membrane-less technologies.[126] It avoids membrane-related issues and simplifies the cell assembly, offering another interesting direction for water electrolysis.

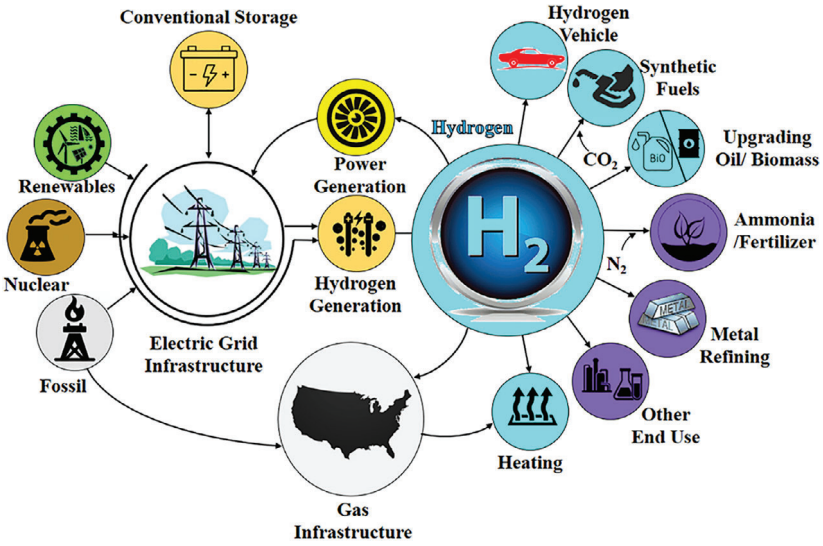

Figure 18. The U.S. hydrogen ecosystem, similar to that of other countries. Reproduced with permission.[120] Copyright 2020, John Wiley & Sons Ltd.

To realize the industrialization of water electrolysis, the cost of electricity remains the most significant factor in green H_2 production. In addition, this cost fluctuates, making the challenge even more difficult. To reduce the cost of electricity, research is being carried out into the coupling of electrolyzers and renewable energies, to take advantage of their overproduction during periods of low demand. To achieve this last objective, extensive weather forecasting is required to anticipate fluctuations. Thus, the primary objective must be clean and low-cost electricity production.

Acknowledgements

A.B. and Z.C. contributed equally to this work. This work was supported by the Natural Sciences and Engineering Research Council of Canada (NSERC), the Fonds de Recherche du Québec-Nature et Technologies (FRQNT), Centre Québécois sur les Materiaux Fonctionnels (CQMF), Réseau québécois sur l'énergie intelligente (RQEI), and École de Technologie Supérieure (ÉTS), Institut National de la Recherche Scientifique (INRS), and IMT Mines Albi (France). A. Bodard acknowledges the support of the Mitacs Globalink program of Canada. Dr. G. Zhang thanks for the support from the Marcelle-Gauvreau Engineering Research Chair program.

Conflict of Interest

The authors declare no conflict of interest.

Keywords

AEM, electrolyzers, fuel cells, green hydrogen, PEM, regenerative fuel cells, renewable energy

Received: April 22, 2024
Revised: September 3, 2024
Published online:

[1] M. Grousson, L'origine humaine du réchauffement fait officiellement consensus depuis au moins 15 ans, https://lejournal.cnrs.fr/articles/lorigine-humaine-du-rechauffement-fait-officiellement-consensus-depuis-au-moins-15-ans (accessed: June, 2024).
[2] Enovate, Net Zero Tracker | Welcome, https://zerotracker.net/ (accessed: June, 2024).
[3] IEA, *Net Zero by 2050 A Roadmap for the Global Energy Sector, IEA*, October **2021**,
[4] IEA, *Global Hydrogen Review 2022*, IEA, September, **2022**.
[5] a) Hydrogène vert, https://www.quebec.ca/agriculture-environnement-et-ressources-naturelles/energie/production-approvisionnement-distribution/hydrogene-vert, (accessed: June, 2024); b) M. Buisine, Infographie : les couleurs de l'hydrogène, https://www.techniques-ingenieur.fr/actualite/articles/infographie-les-couleurs-de-lhydrogene-115418/, (accessed: June, 2024).
[6] a) H. a. F. C. T. Office, Hydrogen Production: Electrolysis, https://www.energy.gov/eere/fuelcells/hydrogen-production-electrolysis (accessed: June, 2024); b) https://www.connaissancedesenergies.org/tribune-actualite-energies/lhydrogene-sera-vraiment-revolutionnaire-sil-est-produit-partir-des-renouvelables (accessed: June, 2024).
[7] a) CAPTAGE DU CO_2, https://www.techniques-ingenieur.fr/glossaire/captage-du-co2 (accessed: June, 2024); b) L. Raynal, S. Tebianian, Captage et stockage du CO2 dans le contexte de la transition énergétique, https://www.techniques-ingenieur.fr/base-documentaire/energies-th4/stockage-de-l-energie-42638210/captage-et-stockage-du-co2-dans-le-contexte-de-la-transition-energetique-be8091/, (accessed: June, 2024); c) S. Pierre, B. Alix, *Impact climatique de l'hydrogène "bleu"*, ADEME Presse, France **2022**.
[8] J. Verne, https://fr.wikisource.org/wiki/Page:Jules_Verne_-_L%E2%80%99%C3%8Ele_myst%C3%A9rieuse.djvu/318 (accessed: June, 2024).
[9] J.-M. Jancovici, presented at *HEC Débats*, Jouy-en-Josas, February, 2020.
[10] O. Chudaev, L. Truche, E. F. Bazarkina, Y. Kharaka, R. Harmon, R. Millot, O. Shouakar-Stash, *E3S Web of Conferences* **2019**, *98*, 00001.
[11] a) T. Talbi, https://www.bfmtv.com/economie/entreprises/energie/qu-est-ce-que-l-hydrogene-blanc-dont-un-gisement-colossal-vient-d-etre-decouvert-en-moselle_AV-202306090505.html (accessed: June, 2024); b) H. Poirier, https://www.francetvinfo.fr/replay-radio/le-billet-sciences-du-week-end/hydrogene-blanc-l-energie-que-personne-n-attendait_5758394.html (accessed: June, 2024).
[12] T. J. Wallington, M. Woody, G. M. Lewis, G. A. Keoleian, E. J. Adler, J. R. R. A. Martins, M. D. Collette, *Joule* **2024**.
[13] U.S. National Clean Hydrogen Strategy and Roadmap, https://www.hydrogen.energy.gov/library/roadmaps-vision/clean-hydrogen-strategy-roadmap, (accessed: June, 2024).
[14] J. S. Hill, Spanish renewable production exceeds 100 pct of country's demand for 9 hours, https://reneweconomy.com.au/spanish-renewable-production-exceeds-100-pct-of-demand-for-9-hours/, (accessed: June, 2024).
[15] a) Déperditions d'énergies ou pertes en ligne: un phénomène naturel, https://www.rte-france.com/riverains/deperditions-denergies-ou-pertes-en-ligne-un-phenomene-naturel (accessed: June, 2024); b) IRENA, *Green Hydrogen Cost Reduction: Scaling up Electrolysers to Meet the 1.5 ^{0}C Climate Goal*, I. R. E. Agency **2020**, December.
[16] C. Rozain, *Ph. D. Thesis*, Université Paris Sud – Paris XI, September, **2013**.
[17] A. Pozio, F. Bozza, G. Nigliaccio, M. Platter, G. Monteleone, *ENEA* **2021**, 66.
[18] a) F. Brissaud, Le Power-to-Gas – Technologies, https://www.techniques-ingenieur.fr/base-documentaire/energies-th4/stockage-de-l-energie-42638210/le-power-to-gas-be6700/#:~:text=Power%2Dto%2DGas%20is%20the,2%20)%20from%20electricity%20and%20water., (accessed: June, 2024); b) C. Li, J.-B. Baek, *Nano Energy* **2021**, *87*, 106162.
[19] a) Z. Zakaria, S. K. Kamarudin, *Int. J. Energy Res.* **2021**, *45*, 18337; b) A. Manabe, M. Kashiwase, T. Hashimoto, T. Hayashida, A. Kato, K. Hirao, I. Shimomura, I. Nagashima, *Electrochim. Acta* **2013**, *100*, 249.
[20] a) IEA, *The Future of Hydrogen: Seizing today's opportunities*, OECD, Paris **2019**; b) IRENA, *Hydrogen from renewable power: Technology outlook for the energy transition*, I. R. E. Agency **2018**, September,
[21] S. Shiva Kumar, V. Himabindu, *Mater. Sci. Energy Technol.* **2019**, *2*, 442.
[22] M. Chatenet, B. G. Pollet, D. R. Dekel, F. Dionigi, J. Deseure, P. Millet, R. D. Braatz, M. Z. Bazant, M. Eikerling, I. Staffell, P. Balcombe, Y. Shao-Horn, H. Schafer, *Chem. Soc. Rev.* **2022**, *51*, 4583.
[23] C. Hu, H. W. Kang, S. W. Jung, M. L. Liu, Y. J. Lee, J. H. Park, N. Y. Kang, M. G. Kim, S. J. Yoo, C. H. Park, Y. M. Lee, *Adv. Sci.* **2024**, *11*, 2306988.
[24] X. W. Lv, W. W. Tian, Z. Y. Yuan, *Electrochem. Energy Rev.* **2023**, *6*, 23.

[25] J. Zhu, L. Hu, P. Zhao, L. Y. S. Lee, K. Y. Wong, *Chem. Rev.* **2020**, *120*, 851.
[26] a) Z. Shi, X. Zhang, X. Lin, G. Liu, C. Ling, S. Xi, B. Chen, Y. Ge, C. Tan, Z. Lai, Z. Huang, X. Ruan, L. Zhai, L. Li, Z. Li, X. Wang, G. H. Nam, J. Liu, Q. He, Z. Guan, J. Wang, C. S. Lee, A. R. J. Kucernak, H. Zhang, *Nature* **2023**, *621*, 300; b) Y. Zhu, M. Klingenhof, C. Gao, T. Koketsu, G. Weiser, Y. Pi, S. Liu, L. Sui, J. Hou, J. Li, H. Jiang, L. Xu, W. H. Huang, C. W. Pao, M. Yang, Z. Hu, P. Strasser, J. Ma, *Nat. Commun.* **2024**, *15*, 1447; c) A. Goyal, S. Louisia, P. Moerland, M. T. M. Koper, *J. Am. Chem. Soc.* **2024**, *146*, 7305; d) X. Liu, Y. Zhou, J. Lin, X. Xiao, Z. Wang, L. Jia, M. Li, K. Yang, J. Fan, W. Yang, G. Li, *Angew. Chem. Int. Ed. Engl.* **2024**, *63*, 202406650.
[27] a) H. Zhu, Y. Wang, Z. Jiang, B. Deng, Y. Xin, Z. J. Jiang, *Adv. Energy Mater.* **2024**; b) Y. Liu, L. Li, L. Wang, N. Li, X. Zhao, Y. Chen, T. Sakthivel, Z. Dai, *Nat. Commun.* **2024**, *15*, 2851; c) B. Lu, C. Wahl, R. dos Reis, J. Edgington, X. K. Lu, R. Li, M. E. Sweers, B. Ruggiero, G. T. K. K. Gunasooriya, V. Dravid, L. C. Seitz, *Nat. Catal.* **2024**.
[28] a) W. Chen, W. Wei, F. Li, Y. Wang, M. Liu, S. Dong, J. Cui, Y. Zhang, R. Wang, K. Ostrikov, S. Q. Zang, *Adv. Funct. Mater.* **2023**, *34*; b) Y. Duan, L. L. Wang, W. X. Zheng, X. L. Zhang, X. R. Wang, G. J. Feng, Z. Y. Yu, T. B. Lu, *Angew. Chem. Int. Ed. Engl.* **2024**, 202413653; c) B. Zhang, J. Wang, G. Liu, C. M. Weiss, D. Liu, Y. Chen, L. Xia, P. Zhou, M. Gao, Y. Liu, J. Chen, Y. Yan, M. Shao, H. Pan, W. Sun, *Nat. Catal.* **2024**, *7*, 441; d) L. Tao, F. Lv, D. W. Wang, H. Luo, F. X. Lin, H. Y. Gong, H. T. Mi, S. G. Wang, Q. H. Zhang, L. Gu, M. C. Luo, S. J. Guo, *Joule* **2024**, *8*, 450.
[29] X. Xu, K. Guo, J. Sun, X. Yu, X. Miao, W. Lu, L. Jiao, *Adv. Funct. Mater.* **2024**, *34*.
[30] Z. Liang, D. Shen, Y. Wei, F. Sun, Y. Xie, L. Wang, H. Fu, *Adv. Mater.* **2024**, 2408634.
[31] H. Huang, L. Xu, S. Zuo, L. Song, C. Zou, M. Garcia-Melchor, Y. Li, Y. Ren, M. Rueping, H. Zhang, *Adv. Mater.* **2024**, 2405128.
[32] a) Z. H. Li, G. X. Lin, L. Q. Wang, H. Lee, J. Du, T. Tang, G. H. Ding, R. Ren, W. L. Li, X. Cao, S. W. Ding, W. T. Ye, W. X. Yang, L. C. Sun, *Nat. Catal.* **2024**; b) J. Nie, J. Shi, T. Huang, M. Y. Xie, Z. Y. Ouyang, M. H. Xian, G. F. Huang, H. Wan, W. Hu, W. Q. Huang, *Adv. Funct. Mater.* **2024**, *34*, 2314172.
[33] R. L. Fan, C. H. Liu, Z. H. Li, H. T. Huang, J. Y. Feng, Z. S. Li, Z. G. Zou, *Nat. Sustain.* **2024**, *7*, 158.
[34] S. Yang, Z. Zhang, A. M. Oliveira, S. Xi, M. Zhiani, J. Zhang, Z. Tu, F. Xiao, S. Wang, Y. Yan, J. Xiao, *Adv. Funct. Mater.* **2024**, *34*, 2313275.
[35] C. Liu, K. Wippermann, M. Rasinski, Y. Suo, M. Shviro, M. Carmo, W. Lehnert, *ACS Appl. Mater. Interfaces* **2021**, *13*, 16182.
[36] a) Q. Wu, Y. Wang, K. Zhang, Z. Xie, K. Sun, W. An, X. Liang, X. Zou, *Mater. Chem. Front.* **2023**, *7*, 1025; b) R. M. Soriano, N. Rojas, E. Nieto, R. de Guadalupe González-Huerta, J. M. Sandoval-Pineda, *Int. J. Hydrogen Energy* **2021**, *46*, 25944.
[37] X. Sun, K. Xu, C. Fleischer, X. Liu, M. Grandcolas, R. Strandbakke, T. Bjørheim, T. Norby, A. Chatzitakis, *Catalysts* **2018**, *8*, 657.
[38] a) M. T. Castro, J. M. Mora, N. Kakati, P.-Y. A. Chuang, J. D. Ocon, *Energy Convers. Manage.* **2022**, *267*, 115829; b) V. Charles, A. O. Anumah, K. A. Adegoke, M. O. Adesina, I. P. Ebuka, N. A. Gaya, S. Ogwuche, M. O. Yakubu, *Sustain. Mater. Technol.* **2021**, *28*, e00252; c) N. T. Suen, S. F. Hung, Q. Quan, N. Zhang, Y. J. Xu, H. M. Chen, *Chem. Soc. Rev.* **2017**, *46*, 337.
[39] Z. Pu, T. Liu, G. Zhang, H. Ranganathan, Z. Chen, S. Sun, *ChemSusChem* **2021**, *14*, 4636.
[40] F.-Y. Chen, Z.-Y. Wu, Z. Adler, H. Wang, *Joule* **2021**, *5*, 1704.
[41] R. Qin, G. Chen, X. Feng, J. Weng, Y. Han, *Adv. Sci. (Weinh)* **2024**, *11*, 2309364.
[42] a) F. Hegge, F. Lombeck, E. Cruz Ortiz, L. Bohn, M. von Holst, M. Kroschel, J. Hübner, M. Breitwieser, P. Strasser, S. Vierrath, *ACS Appl. Energy Mater.* **2020**, *3*, 8276; b) G. Mirshekari, R. Ouimet, Z. Zeng, H. Yu, S. Bliznakov, L. Bonville, A. Niedzwiecki, C. Capuano, K. Ayers, R. Maric, *Int. J. Hydrogen Energy* **2021**, *46*, 1526; c) S. A. Grigoriev, A. A. Kalinnikov, *Int. J. Hydrogen Energy* **2017**, *42*, 1590.
[43] H. Yu, N. Danilovic, Y. Wang, W. Willis, A. Poozhikunnath, L. Bonville, C. Capuano, K. Ayers, R. Maric, *Appl. Catal., B* **2018**, *239*, 133.
[44] S. Du, R. Chen, W. Chen, H. Gao, J. Jia, Z. Xiao, C. Xie, H. Li, L. Tao, J. Huo, Y. Wang, S. Wang, *J. Energy Chem.* **2022**, *75*, 260.
[45] C. Hao, H. Lv, C. Mi, Y. Song, J. Ma, *ACS Sustainable Chem. Eng.* **2015**, *4*, 746.
[46] E.-J. Kim, J. Shin, J. Bak, S. J. Lee, K. h. Kim, D. Song, J. Roh, Y. Lee, H. Kim, K.-S. Lee, E. Cho, *Appl. Catal., B* **2021**, *280*, 119433.
[47] Q. Jia, E. Liu, L. Jiao, J. Li, S. Mukerjee, *Curr. Opin. Electrochem.* **2018**, *12*, 209.
[48] L. é. chimiques, Abondance dans la croute terrestre, https://www.elementschimiques.fr/?fr/proprietes/abondances/abondance-dans-la-croute-terrestre, (accessed: June, **2024**).
[49] D. M. Prices, Ruthenium Prices for the Last 10 Years, https://www.dailymetalprice.com/metalpricecharts.php?c=ru&u=oz&d=2400, (accessed: June, 2024).
[50] a) D. M. Prices, Platinum Prices for the Last 10 Years, https://www.dailymetalprice.com/metalpricecharts.php?c=pt&u=oz&d=240, (accessed: June, 2024); b) D. M. Prices, Palladium Prices for the Last 10 Years, https://www.dailymetalprice.com/metalpricecharts.php?c=pd&u=oz&d=240, (accessed: June, 2024).
[51] a) P. Serp, D. P. Minh, *Supported Metal Single Atom Catalysis*, John Wiley and Sons, Weinheim, Germany **2022**; b) X. F. Yang, A. Wang, B. Qiao, J. Li, J. Liu, T. Zhang, *Acc. Chem. Res.* **2013**, *46*, 1740.
[52] Z. Pu, T. Liu, G. Zhang, Z. Chen, D. S. Li, N. Chen, W. Chen, Z. Chen, S. Sun, *Adv. Energy Mater.* **2022**, *12*, 2200293.
[53] Y. Zhu, J. Wang, H. Chu, Y.-C. Chu, H. M. Chen, *ACS Energy Lett.* **2020**, *5*, 1281.
[54] C. Santoro, A. Lavacchi, P. Mustarelli, V. Di Noto, L. Elbaz, D. R. Dekel, F. Jaouen, *ChemSusChem* **2022**, *15*, 202200027.
[55] K. Zhang, X. Liang, L. Wang, K. Sun, Y. Wang, Z. Xie, Q. Wu, X. Bai, M. S. Hamdy, H. Chen, X. Zou, *Nano Research Energy* **2022**, *1*, 9120032.
[56] a) J. Knoppel, M. Mockl, D. Escalera-Lopez, K. Stojanovski, M. Bierling, T. Bohm, S. Thiele, M. Rzepka, S. Cherevko, *Nat. Commun.* **2021**, *12*, 2231; b) K. Ehelebe, D. Escalera-López, S. Cherevko, *Curr. Opin. Electrochem.* **2021**, *29*, 100832.
[57] L.-Y. Zhu, Y.-C. Li, J. Liu, J. He, L.-Y. Wang, J.-D. Lei, *Petroleum Sci.* **2022**, *19*, 1371.
[58] B. Guenot, Univ. Montpellier, **2017**.
[59] F. Barbir, *Sol. Energy* **2005**, *78*, 661.
[60] T. Inoue, M. A. Schmidt, K. F. Jensen, *Ind. Eng. Chem. Res.* **2007**, *46*, 1153.
[61] L. Ma, S. Sui, Y. Zhai, *Int. J. Hydrogen Energy* **2009**, *34*, 678.
[62] S. Bukola, S. E. Creager, *ECS Trans.* **2019**, *92*, 439.
[63] a) C. Klose, P. Trinke, T. Böhm, B. Bensmann, S. Vierrath, R. Hanke-Rauschenbach, S. Thiele, *J. Electrochem. Soc.* **2018**, *165*, F1271; b) S. Garbe, U. Babic, E. Nilsson, T. J. Schmidt, L. Gubler, *J. Electrochem. Soc.* **2019**, *166*, F873.
[64] a) M. Chandesris, V. Médeau, N. Guillet, S. Chelghoum, D. Thoby, F. Fouda-Onana, *Int. J. Hydrogen Energy* **2015**, *40*, 1353; b) Q. Feng, X. Z. Yuan, G. Liu, B. Wei, Z. Zhang, H. Li, H. Wang, *J. Power Sources* **2017**, *366*, 33.
[65] a) G. Papakonstantinou, G. Algara-Siller, D. Teschner, T. Vidaković-Koch, R. Schlögl, K. Sundmacher, *Appl. Energy* **2020**, *280*, 115911; b) S. Siracusano, V. Baglio, N. Briguglio, G. Brunaccini, A. Di Blasi, A. Stassi, R. Ornelas, E. Trifoni, V. Antonucci, A. S. Aricò, *Int. J. Hydrogen Energy* **2012**, *37*, 1939; c) S. Sun, Z. Shao, H. Yu, G. Li, B. Yi, *J. Power Sources* **2014**, *267*, 515.
[66] M. Carmo, D. L. Fritz, J. Mergel, D. Stolten, *Int. J. Hydrogen Energy* **2013**, *38*, 4901.

[67] J. E. Park, J. Kim, J. Han, K. Kim, S. Park, S. Kim, H. S. Park, Y.-H. Cho, J.-C. Lee, Y.-E. Sung, *J. Membr. Sci.* **2021**, *620*, 118871.
[68] a) D. Choi, *Membranes (Basel)* **2022**, *12*; b) H. Ito, T. Maeda, A. Nakano, H. Takenaka, *Int. J. Hydrogen Energy* **2011**, *36*, 10527.
[69] a) S. Jang, Y. S. Kang, J. Choi, J. H. Yeon, C. Seol, L. V. Nam, M. Choi, S. M. Kim, S. J. Yoo, *J. Indust. Engineer. Chem.* **2020**, *90*, 327; b) N. Wehkamp, M. Breitwieser, A. Büchler, M. Klingele, R. Zengerle, S. Thiele, *RSC Adv.* **2016**, *6*, 24261; c) V. Antonucci, A. Di Blasi, V. Baglio, R. Ornelas, F. Matteucci, J. Ledesma-Garcia, L. G. Arriaga, A. S. Aricò, *Electrochim. Acta* **2008**, *53*, 7350.
[70] Q. Xu, L. Zhang, J. Zhang, J. Wang, Y. Hu, H. Jiang, C. Li, *EnergyChem* **2022**, *4*, 100087.
[71] H. Cheng, H. Luo, X. Wang, Z. Pan, Q. Zhao, C. Dong, X. Li, *Int. J. Hydrogen Energy* **2023**, *48*, 38557.
[72] J.-H. Choi, H. E. Kang, D.-J. Kim, Y. S. Yoon, *Chem. Eng. J.* **2024**, *493*, 152662.
[73] L. Messing, K. Pellumbi, L. Hoof, N. Imming, S. Wilbers, L. Kopietz, M. Joemann, A. Grevé, K. junge Puring, U. P. Apfel, *Adv. Energy Mater.* **2024**.
[74] X.-Z. Yuan, N. Shaigan, C. Song, M. Aujla, V. Neburchilov, J. T. H. Kwan, D. P. Wilkinson, A. Bazylak, K. Fatih, *Sustain. Energy Fuels* **2022**, *6*, 1824.
[75] S. Yuan, C. Zhao, X. Cai, L. An, S. Shen, X. Yan, J. Zhang, *Prog. Energy Combust. Sci.* **2023**, *96*, 101075.
[76] P. Holzapfel, M. Bühler, C. Van Pham, F. Hegge, T. Böhm, D. McLaughlin, M. Breitwieser, S. Thiele, *Electrochem. Commun.* **2020**, *110*, 106640.
[77] a) A. Laube, A. Hofer, B. Sánchez Batalla, S. Ressel, A. Chica, S. Fischer, C. Weidlich, J. Bachmann, T. Struckmann, *Int. J. Hydrogen Energy* **2022**, *47*, 15943; b) W. Xu, K. Scott, *Int. J. Hydrogen Energy* **2010**, *35*, 12029.
[78] M. Bühler, P. Holzapfel, D. McLaughlin, S. Thiele, *J. Electrochem. Soc.* **2019**, *166*, F1070.
[79] a) M. Breitwieser, M. Klingele, B. Britton, S. Holdcroft, R. Zengerle, S. Thiele, *Electrochem. Commun.* **2015**, *60*, 168; b) M. Stähler, A. Stähler, F. Scheepers, M. Carmo, D. Stolten, *Int. J. Hydrogen Energy* **2019**, *44*, 7053.
[80] M. N. I. Salehmin, T. Husaini, J. Goh, A. B. Sulong, *Energy Convers. Manage.* **2022**, *268*, 115985.
[81] C. V. Pham, D. Escalera-López, K. Mayrhofer, S. Cherevko, S. Thiele, *Adv. Energy Mater.* **2021**, *11*.
[82] H. J. Park, S. Y. Lee, T. K. Lee, H.-J. Kim, Y. M. Lee, *J. Membr. Sci.* **2020**, *611*, 118355.
[83] a) H. A. Miller, K. Bouzek, J. Hnat, S. Loos, C. I. Bernäcker, T. Weißgärber, L. Röntzsch, J. Meier-Haack, *Sustain. Energy Fuels* **2020**, *4*, 2114; b) K. I. o. S. a. Technology(KIST), Schematic diagram of anhydrous cathode AEMWE and the chemical structures of the PFAP AEMs and ionomers, https://www.eurekalert.org/multimedia/899873, (accessed: June, 2024).
[84] a) A. Loh, X. Li, S. Sluijter, P. Shirvanian, Q. Lai, Y. Liang, *Hydrogen* **2023**, *4*, 257; b) A. W. Tricker, J. K. Lee, J. R. Shin, N. Danilovic, A. Z. Weber, X. Peng, *J. Power Sources* **2023**, *567*, 232967; c) A. Khataee, A. Shirole, P. Jannasch, A. Krüger, A. Cornell, *J. Mater. Chem. A* **2022**, *10*, 16061.
[85] R. R. Raja Sulaiman, W. Y. Wong, K. S. Loh, *Int. J. Energy Res.* **2021**, *46*, 2241.
[86] P. Shirvanian, A. Loh, S. Sluijter, X. Li, *Electrochem. Commun.* **2021**, *132*, 107140.
[87] E. Willinger, C. Massué, R. Schlögl, M. G. Willinger, *J. Am. Chem. Soc.* **2017**, *139*, 12093.
[88] H. Koshikawa, H. Murase, T. Hayashi, K. Nakajima, H. Mashiko, S. Shiraishi, Y. Tsuji, *ACS Catal.* **2020**, *10*, 1886.
[89] M. Klingenhof, P. Hauke, M. Kroschel, X. Wang, T. Merzdorf, C. Binninger, T. Ngo Thanh, B. Paul, D. Teschner, R. Schlögl, P. Strasser, *ACS Energy Lett.* **2022**, *7*, 3415.
[90] a) S. S. Jeon, J. Lim, P. W. Kang, J. W. Lee, G. Kang, H. Lee, *ACS Appl. Mater. Interfaces* **2021**, *13*, 37179; b) J. Xing, Z. Zeng, A. Koni, G. Mirshekari, W. Best, V. Kumar, L. Sammes, L. J. Bonville, R. Maric, S. Bliznakov, *ECS Meeting Abstracts* **2022**, *MA2022-02*, 1389. c) W. Jiang, A. Y. Faid, B. F. Gomes, I. Galkina, L. Xia, C. M. S. Lobo, M. Desmau, P. Borowski, H. Hartmann, A. Maljusch, A. Besmehn, C. Roth, S. Sunde, W. Lehnert, M. Shviro, *Adv. Funct. Mater.* **2022**, *32*; d) J. Zhao, N. Liao, J. Luo, *J. Mater. Chem. A* **2023**, *11*, 9682; e) Y. Zhai, X. Ren, Y. Sun, D. Li, B. Wang, S. Liu, *Appl. Catal., B* **2023**, *323*, 122091.
[91] B. Li, H. Fan, M. Cheng, Y. Song, F. Li, X. Wang, R. Wang, *RSC Adv.* **2018**, *8*, 698.
[92] a) S.-J. Hwang, J.-W. Kim, S.-J. Yoo, J.-H. Jang, E.-A. Cho, T.-H. Lim, S.-G. Pyo, S.-K. Kim, *Bull. Korean Chem. Soc.* **2012**, *33*, 699; b) N. Du, C. Roy, R. Peach, M. Turnbull, S. Thiele, C. Bock, *Chem. Rev.* **2022**, *122*, 11830; c) Q. Li, A. Molina Villarino, C. R. Peltier, A. J. Macbeth, Y. Yang, M.-J. Kim, Z. Shi, M. R. Krumov, C. Lei, G. G. Rodríguez-Calero, J. Soto, S.-H. Yu, P. F. Mutolo, L. Xiao, L. Zhuang, D. A. Muller, G. W. Coates, P. Zelenay, H. D. Abruña, *J. Phys. Chem. C* **2023**, *127*, 7901.
[93] H. A. Miller, *Curr. Opin. Electrochem.* **2022**, *36*, 101122.
[94] P. Chen, X. Hu, *Adv. Energy Mater.* **2020**, *10*.
[95] F. Bartoli, L. Capozzoli, T. Peruzzolo, M. Marelli, C. Evangelisti, K. Bouzek, J. Hnát, G. Serrano, L. Poggini, K. Stojanovski, V. Briega-Martos, S. Cherevko, H. A. Miller, F. Vizza, *J. Mater. Chem. A* **2023**, *11*, 5789.
[96] J. Zhang, T. Wang, P. Liu, Z. Liao, S. Liu, X. Zhuang, M. Chen, E. Zschech, X. Feng, *Nat. Commun.* **2017**, *8*, 15437.
[97] M. Ďurovič, J. Hnát, K. Bouzek, *J. Power Sources* **2021**, *493*, 229708.
[98] G. Ding, H. Lee, Z. Li, J. Du, L. Wang, D. Chen, L. Sun, *Adv. Energy Sustain. Res.* **2022**, *4*.
[99] a) S. Hong, H. Kim, H. W. Jang, S. Y. Kim, S. H. Ahn, *Dalton Trans.* **2023**, *52*, 6324; b) M. P. H. Klingenhof, *Ph.D. Thesis*, Technischen Universität Berlin, **2022**; c) P. Wang, Y. Luo, G. Zhang, M. Wu, Z. Chen, S. Sun, Z. Shi, *Small* **2022**, *18*, 2105803.
[100] Y. Luo, P. Wang, G. Zhang, S. Wu, Z. Chen, H. Ranganathan, S. Sun, Z. Shi, *Chem. Eng. J.* **2023**, *454*, 140061.
[101] R. Vinodh, S. S. Kalanur, S. K. Natarajan, B. G. Pollet, *Polymers (Basel)* **2023**, *15*.
[102] N. Chen, S. Y. Paek, J. Y. Lee, J. H. Park, S. Y. Lee, Y. M. Lee, *Energy Environ. Sci.* **2021**, *14*, 6338.
[103] M. Bernt, H. A. Gasteiger, *J. Electrochem. Soc.* **2016**, *163*, F3179.
[104] D. Li, A. R. Motz, C. Bae, C. Fujimoto, G. Yang, F.-Y. Zhang, K. E. Ayers, Y. S. Kim, *Energy Environ. Sci.* **2021**, *14*, 3393.
[105] D. Materials, Contribution To The Hydrogen Economy, https://dioxidematerials.com/applications/dioxide-materials-contribution-hydrogen-economy/, (accessed: 2024).
[106] R. B. Kutz, Q. Chen, H. Yang, S. D. Sajjad, Z. Liu, I. R. Masel, *Energy Technol.* **2017**, *5*, 929.
[107] M. A. Khan, I. Al-Shankiti, A. Ziani, H. Idriss, *Sustainable Energy Fuels* **2021**, *5*, 1085.
[108] J. E. Park, S. Y. Kang, S.-H. Oh, J. K. Kim, M. S. Lim, C.-Y. Ahn, Y.-H. Cho, Y.-E. Sung, *Electrochim. Acta* **2019**, *295*, 99.
[109] J. E. Park, H. J. Choi, S. Y. Kang, G. Y. Jang, O. H. Kim, M. Karuppannan, Y. E. Sung, O. J. Kwon, Y. H. Cho, *Int. J. Energy Res.* **2022**, *46*, 16670.
[110] A. H. Faqeeh, M. D. Symes, *Electrochim. Acta* **2023**, *444*, 142030.
[111] L. Wan, Z. Xu, B. Wang, *Chem. Eng. J.* **2021**, *426*, 131340.

[112] Enapter, Enapter AEM Electrolysers: Produce maximum green hydrogen from renewables, https://www.enapter.com/, (accessed: 2024).
[113] R. Omrani, B. Shabani, *Int. J. Hydrogen Energy* **2019**, *44*, 3834.
[114] H. Rezk, S. Ferahtia, A. Djeroui, A. Chouder, A. Houari, M. Machmoum, M. A. Abdelkareem, *Energy* **2022**, *239*, 122096.
[115] M. Horlacher, Pile à combustible, https://h2sys.fr/technologies/pile-a-combustible/, (accessed: June, 2024).
[116] a) I. E. Agency, *Technology Roadmap Hydrogen and Fuel Cells*, CORLET, , **2015**, b) M. A. Abdelkareem, K. Elsaid, T. Wilberforce, M. Kamil, E. T. Sayed, A. Olabi, *Sci. Total Environ.* **2021**, *752*, 141803; c) H. a. F. C. T. Office, Comparison of Fuel Cell Technologies, https://www.energy.gov/eere/fuelcells/comparison-fuel-cell-technologies, (accessed: June, 2024). d) Z. H. Pu, G. X. Zhang, A. Hassanpour, D. W. Zheng, S. Y. Wang, S. J. Liao, Z. X. Chen, S. H. Sun, *Appl. Energy* **2021**, *283*, 116376; e) F. Lamari, P. Langlois, P. Malbrunot, Combustible hydrogène – Utilisation, https://www.techniques-ingenieur.fr/base-documentaire/energies-th4/stockage-de-l-energie-42638210/combustible-hydrogene-be8566/conversion-energetique-de-l-hydrogene-be8566v3niv10001.html, (accessed: June, 2024).
[117] a) S. Gottesfeld, D. R. Dekel, M. Page, C. Bae, Y. Yan, P. Zelenay, Y. S. Kim, *J. Power Sources* **2018**, *375*, 170; b) J. E. Chae, S. Y. Lee, S. J. Yoo, J. Y. Kim, J. H. Jang, H. Y. Park, H. S. Park, B. Seo, D. Henkensmeier, K. H. Song, H. J. Kim, *Polymers* **2021**, *13*.
[118] Y. N. Regmi, X. Peng, J. C. Fornaciari, M. Wei, D. J. Myers, A. Z. Weber, N. Danilovic, *Energy Environ. Sci.* **2020**, *13*, 2096.
[119] Y. Wang, D. Y. C. Leung, J. Xuan, H. Wang, *Renew. Sustain. Energy Rev.* **2016**, *65*, 961.
[120] A. A. Salehi, M. Ghannadi-Maragheh, M. Torab-Mostaedi, R. Torkaman, M. Asadollahzadeh, *Int. J. Energy Res.* **2020**, *45*, 11423.
[121] H. a. F. C. T. Office, H2@Scale, https://www.energy.gov/eere/fuelcells/h2scale (accessed: June, 2024).
[122] a) M. Camacho, D. Jurburg, M. Tanco, *Int. J. Hydrogen Energy* **2022**, *47*, 29505; b) H. Kouchaki-Penchah, O. Bahn, H. Bashiri, S. Bedard, E. Bernier, T. Elliot, A. Hammache, K. Vaillancourt, A. Levasseur, *Int. J. Hydrogen Energy* **2024**, *49*, 173.
[123] P. Segal, Midstream's Growing Role in Clean Hydrogen, https://www.etftrends.com/energy-infrastructure-channel/midstreams-growing-role-in-clean-hydrogen/, (accessed: August, 2024).
[124] B. Weetch, First Hydrogen to develop green hydrogen ecosystem in Quebec, https://www.globalhydrogenreview.com/hydrogen/28112022/first-hydrogen-to-develop-green-hydrogen-ecosystem-in-quebec/, (accessed: August, 2024).
[125] J. N. Hausmann, L. R. Winter, M. A. Khan, M. Elimelech, M. G. Kibria, T. Sontheimer, P. W. Menezes, *Joule* **2024**.
[126] D. V. Esposito, *Joule* **2017**, *1*, 651.

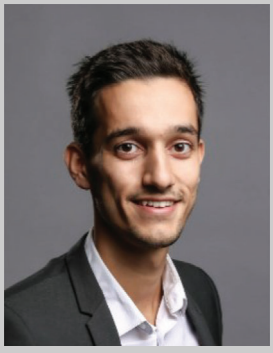

Alexandre Bodard is a general engineer who graduated from IMT Mines Albi, France, in 2024, with a degree in "conversion, distribution and production of clean energy". He undertook a research internship on green hydrogen production through electrolysis at ÉTS Montreal, Canada, under the supervision of Prof. Gaixia Zhang. He then completed a second internship as an engineer focusing on industrial hydrogen projects at Hynamics in Paris, a subsidiary of the EDF group specializing in hydrogen initiatives.

Zhangsen Chen obtained his B.S. degree at Fuzhou University in 2014, followed by a master's degree in physical chemistry from the Research Institute of Photocatalysis, Fuzhou University, in 2017. He completed his Ph.D. degree in energy and material science at the Institut National de la Recherche Scientifique (INRS), University of Québec, in 2023. Currently, he is a postdoctoral fellow at INRS. His research interests focus on the development of advanced nanomaterials and their applications in H_2 production and CO_2 conversion into value-added chemicals and fuels.

Gaixia Zhang is a professor and Marcelle-Gauvreau Engineering Research Chair at École de Technologie Supérieure (ÉTS), University of Quebec, Montréal, Canada. She received her Ph.D. degree from Polytechnique Montréal, and then continued her research at Western University and INRS, Canada. Her research interests focus on advanced materials (catalysts, electrodes and electrolytes) for sustainable energy conversion and storage applications, including batteries, fuel cells, hydrogen production, and CO_2 reduction. She is also interested in interface and device engineering, as well as in-situ characterizations and theoretical simulations.